Review

Advanced oxidation processes for the removal of mono and polycyclic aromatic hydrocarbons – A review

Manoj P. Rayaroth [a,b], Mateusz Marchel [a], Grzegorz Boczkaj [c,d,*]

[a] Gdańsk University of Technology, Faculty of Chemistry, Department of Process Engineering and Chemical Technology, 80-233 Gdańsk, G. Narutowicza 11/12 Str, Poland
[b] GREMI, UMR 7344, Université d'Orléans, CNRS, 45067 Orléans, France
[c] Gdańsk University of Technology, Faculty of Civil and Environmental Engineering, Department of Sanitary Engineering, 80-233 Gdańsk, G. Narutowicza 11/12 Str, Poland
[d] EkoTech Center, Gdansk University of Technology, G. Narutowicza St. 11/12, 80-233 Gdansk, Poland

HIGHLIGHTS

- Fast degradation of monocyclic aromatics, BTEX vs slow for PAHs.
- Solubilization assisted oxidation is effective for PAHs removal from soil.
- Advantageous presence of carbonates for degradation of PAHs derivatives.
- Significance of radical based mechanisms of aromatic hydrocarbons decomposition.
- SR-AOPs are favorable for soil remediation of PAHs.

GRAPHICAL ABSTRACT
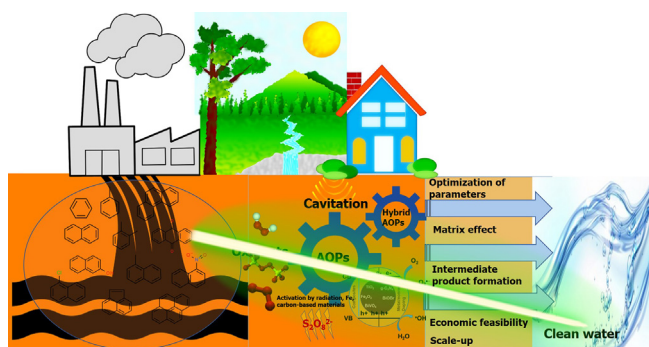
ARTICLE INFO

ABSTRACT

Aromatic hydrocarbons (AHs) are toxic environmental contaminants presented in most of the environmental matrices. Advanced oxidation processes (AOPs) for the removal of AHs in the account of complete mineralization from various environmental matrices have been reviewed in this paper. An in-depth discussion on various AOPs for mono (BTEX) and polyaromatic hydrocarbons (PAHs) and their derivatives is presented. Most of the AOPs were effective in the removal of AHs from the aquatic environment. A comparative study on the degradation of various AHs revealed that the oxidation of the AHs is strongly dependent on the number of aromatic rings and the functional groups attached to the ring. The formation of halogenated and nitrated derivatives of AHs in the real contaminated water containing chloride, nitrite, and nitrate ions seems to be a challenge in using the AOPs in real systems. The phenolic compounds, quinone, alcohols, and aliphatic acids are the important byproducts formed during the oxidation of AHs, initiated by the attack of reactive oxygen species (ROS) on their electron-rich center. In conclusion, AOPs are the adaptable method for the removal of AHs from different environmental matrices. The persulfate-based AOPs were applied in the soil phase removal as an in situ chemical oxidation of AHs. Moreover, the combination of AOPs will be a conclusive solution to avoid or minimize unexpected or other toxic intermediate products and to obtain rapid oxidation of AHs.

Contents

1. Introduction

Aromatic hydrocarbons (AHs) have been widely discharged into the natural environment by the partial combustion of organic materials like oil, petroleum products, gas, coal, and wood. Based on the structural feature of the AHs, they can be divided into monocyclic or polycyclic hydrocarbons (PAHs). Among the monocyclic AHs, special attention has been given to BTEX (Benzene, Toluene, Ethylbenzene, and Xylene). On the other hand, PAHs contain fused benzene rings. PAHs can be further classified into light and heavy PAHs based on the number of benzene rings in the structure. The PAHs bearing up to four benzene rings are included in the category of light and more than four rings are included in the group of heavy PAHs (Dhar et al., 2020; Makoś et al., 2018). PAHs are lipophilic in nature, only slightly volatile, and almost insoluble in water. In addition, the lipophilicity of PAHs is directly related to the number of rings in the structure. Most of the PAHs are not synthesized directly for commercial purposes, instead some PAHs like Acenaphthene, Anthracene, Fluoranthene, Fluorene, Phenanthrene, and Pyrene, is used as a precursor in the synthesis of pesticides, pharmaceuticals, dyes, pigments, plastics, etc. (Abdel-Shafy and Mansour, 2016).

Because of the long-term emission of PAHs, their presence in various environmental compartments such as soil, air, and water has been reported. The strong hydrophobic character of PAHs avail them mostly in soil matrices and would act as the sink for PAHs. Combustion of organic materials like oil, petroleum products, gas, coal, and wood leads to the release abundant of PAHs into the air and can undergo wet and dry deposition onto water, soil, and vegetation (Chakraborty et al., 2019; Cheng et al., 2013; Khuman et al., 2018). Moreover, the direct discharge of chemical wastes (extraction, transportation, and refining) from the petrochemical industry leads to the direct contamination of water sources by PAHs (Gao et al., 2019; Zhang et al., 2021). The low water solubility makes them persist in the soil matrix for a long time. The PAHs can enter the living organism through the food chain, skin, or via inhalation and affect the living organism (Agarwal et al., 2022). As a result, the EU and US included this kind of pollutants in the high-priority organic chemicals due to growing environmental and human health concerns (Keith, 2015). Therefore, the removal of this kind of chemical compound from water sources is strongly recommended. In the atmosphere, it may react with the photochemically generated oxidants, reactive oxygen, and nitrogen species (ROS and RNs) to form hydroxylated and nitrated AHs. The nitro, dinitro, nitro-hydroxy, and nitro-oxy AHs are formed in the atmosphere by the reaction with O_3 and nitrogen oxide radicals (Alves et al., 2017). Therefore one should

aware of their transformation product as well. These risks can take place also during wastewater treatment (Rayaroth et al., 2022).

Various technologies have been implemented to remove these contaminants from various water sources to lessen their human exposure. The physical processes, such as adsorption, filtration, flocculation, sedimentation, membrane techniques, etc. were successful in eliminating the PAHs to non-detectable limits. However, their phase change and instability of the materials would cause unexpected effects (Adeola and Forbes, 2021). Therefore, most of the methods focus on the complete mineralization of PAHs in a short period (Gaurav et al., 2021; Rubio-Clemente et al., 2014).

2. Advanced oxidation processes for PAHs degradation

Advanced oxidation processes (AOPs) are one of the most effective methods for the removal of organic contaminants, wherein the *in situ* generated reactive species play a key role in the degradation. A vast variety of pollutants such as dyes, pesticides, endocrine disrupters, and many emerging pollutants were removed and underwent complete mineralization by these processes within a short period. AOPs are a promising group of processes for the complete conversion of target compound to less or non-toxic form and finally to complete mineralization (Boczkaj and Fernandes, 2017; Elmobarak et al., 2021; Srivastav et al., 2019). This advantage is utilized for the degradation of PAHs from both aqueous media and the contaminated site. The physicochemical properties, especially the solubility and hydrophobicity of the AHs increased with an increase in the number of aromatic rings (Lawal, 2017). It is noted that the derivatives of AHs have a variety of functional groups such as -NO₂, -NH₂, -OH, -COOH, SO₃H, N═N, etc. Therefore, their degradation in AOPs mainly depends on these functional groups, where they can direct the reactive species to certain positions of the aromatic ring. Therefore, future studies on their reaction towards the reactive species and the subsequent degradation will be interesting. A detailed literature survey has been done on this topic for PAHs and the number of studies reported is given in Fig. 1. There are many studies related to the pollution of environmental matrices by PAHs and as a result, the researcher is studying their remediation, especially using oxidation processes. As can be seen from Fig. 1 the number of publications for the removal of PAHs using AOPs is increasing every year. In addition, there are some reviews reported which are targeting the removal of AHs (Elmobarak et al., 2021; Ren et al., 2022; Rubio-Clemente et al., 2014; Srivastav et al., 2019). However, these reviews emphasized the removal of either monocyclic AHs or PAHs. On the other hand, only limited information is available for the removal of their transformation products, and the
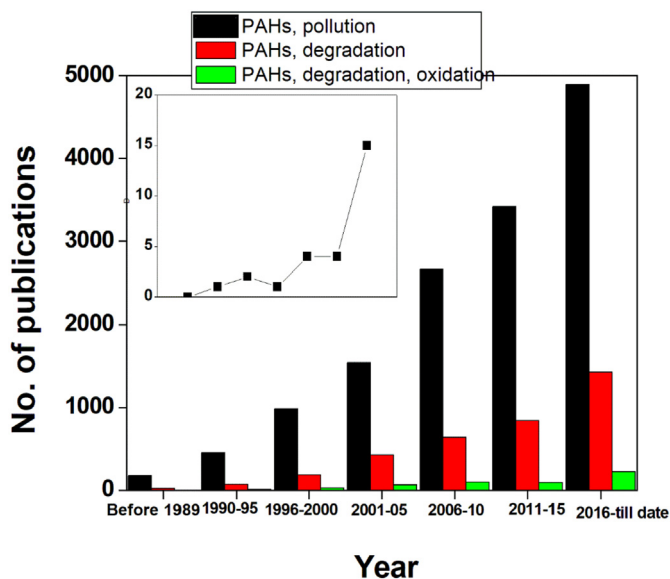
Fig. 1. Number of publications reported for the topic PAHs; the searched keywords in Scopus are given as legends. Inset shows the reviews on the keywords "*PAHs, oxidation, degradation*".

cost of treatment is not specified in most of the review papers. In this aspect, this review discusses various approaches for oxidative degradation for AHs from environmental matrices (Fig. 2).

2.1. UV/oxidant based AOPs for PAHs

The UV-based processes are reported as the fast oxidation method for aromatic compounds. In some cases, pollutants undergo degradation under UV irradiation depending on the photophysical properties of the target compounds. But, UV coupled with oxidants is the most effective method in generating ROS and degrading organic contaminants with lower absorptivity in the UV region. The oxidants used in this process are H_2O_2, O_3, peroxy disulfate (PDS, $S_2O_8^{2-}$), and peroxy monosulfate (PMS, HSO_5^-). The light irradiation would break the peroxide bond in the oxidants to form reactive species like •OH, HO_2•, in the case of UV/H_2O_2, and UV/O_3
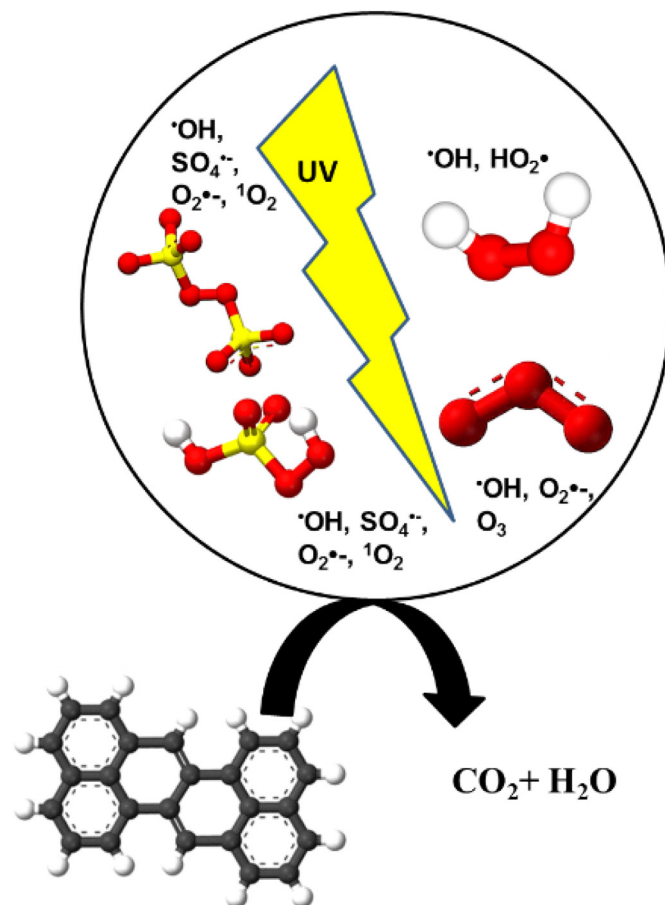
Fig. 3. UV activation of oxidants (PMS, PDS, H_2O_2, and O_3) for the removal of PAHs.

and sulfate radicals in the presence of UV/PDS or PMS (Fig. 3) (Li et al., 2017; Peyton and Glaze, 1988). All these ROS can degrade PAHs.

The UV combined with oxidants for the AHs degradation are given in the supporting information Table S1. The effectiveness of incorporating the H_2O_2 in photolysis was studied by Shemer and Linden (2007a);
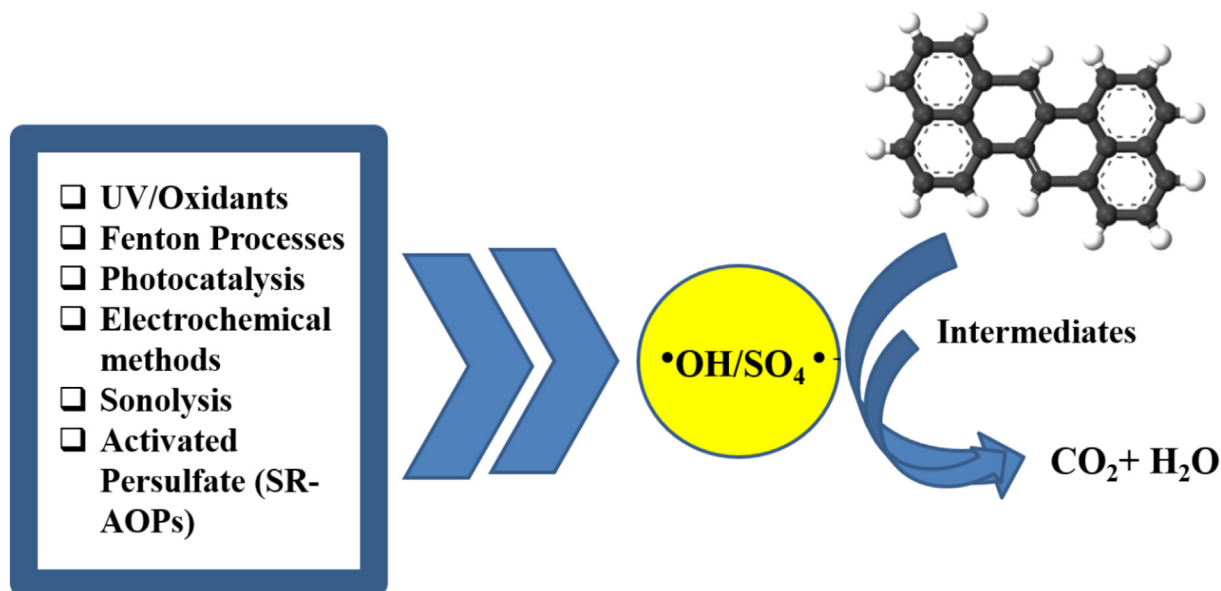
Fig. 2. Various AOPs and SR-AOPs reported for the removal of AHs.

Shemer and Linden (2007b) They investigated the degradation of FLU, dibenzofuran, and dibenzothiophene (DBT) using H_2O_2 in combination with low-pressure monochromatic (LP) and medium pressure polychromatic (MP) UV sources. The degradation was significantly influenced by the addition of H_2O_2, a 36-fold and 109-fold increase in the degradation was observed under LP and MP sources respectively compared to the direct photolysis. With this background, the removal of PAHs from more realistic environmental conditions has been carried out. Various environmentally relevant factors such as solution pH, organics concentration, and matrix composition have been addressed. Bahmani et al. found that UV/H_2O_2 oxidation was effective in the removal of BTEX in real wastewater (Bahmani et al., 2014). In this process, the removal as a function of COD was monitored and 50 % of the COD was reduced. Lhotský et al. also found that 80 % of the BTEX was removed from a mixture of mono aromatic contaminants after 150 min from the groundwater matrix (Lhotský et al., 2017). Bustillo-Lecompte et al. have investigated the degradation of BTEX using UV/H_2O_2 at various oxidant concentrations (Bustillo-Lecompte et al., 2018). More than 60 % of the TOC removal was achieved using both UV-254 and UV-185 sources after 4 h. Biodegradability as the function of BOD_5/TOC was also determined in this study. It is found that the BOD5/ TOC ratio was decreased by 32 % and 21 % during $UV-254/H_2O_2$ and $UV-185/H_2O_2$ process, i.e. a decrease in biodegradability was observed. Thus, they proposed that this process can be used as a post-treatment method when combined with the biological oxidation method. Daifullah et al. noted 90 % degradation in just 10 min using this process (Daifullah and Mohamed, 2004). On the other hand, a literature on light-activated PS for AHs degradation is scarce – this aspect is further commented in Section 2.6.

In summary, the UV/H_2O_2 process successfully removed >90 % of AHs within a short irradiation time. However, the optimization of the H_2O_2 dose to achieve >90 % degradation/COD is an important step in this process. The appropriate UV lamp selection is also necessary for this kind of AOP.

2.2. Fenton and photo-Fenton processes for PAHs

Fenton processes are an important branch in AOPs for the treatment of organic contaminants (Zhang et al., 2019). In this process, the Fe^{2+} ions react with hydrogen peroxide to form ROS. The Fenton reaction occurs between Fe^{2+} and H_2O_2 with the formation of •OH and Fe^{3+}. The generated Fe^{3+} can also be reduced to Fe^{2+} in the presence of H_2O_2. The reaction rate for the oxidation of Fe^{2+} to Fe^{3+} is several thousand times higher than that of the Fe^{3+} reduction. Therefore, the key step is the formation of •OH and the increasing concentration of Fe^{3+} in the aqueous medium. The advantage of the Fenton process is its robustness in the operation. Since Fe^{2+} is regenerated during the reaction, only a small amount of Fe^{2+} is needed. The Fenton-based processes are either homogeneous or heterogeneous depending on the Fe form introduced into the treated solution. The efficiency of the process depends on the $Fe^{2+}:H_2O_2$ ratio and the initial pH of the solution (Zhang et al., 2019). The process is usually more effective in the pH range of 2–3 irrespective of the compound. The reactions involved in Fenton reaction reactions are given in Eqs. (1)–(3).

$$Fe^{2+} + H_2O_2 + H^+ \rightarrow Fe^{3+} + OH^- + HO^\bullet \quad (1)$$

$$Fe^{3+} + H_2O_2 \rightarrow Fe^{2+} + HO_2^\bullet + H^+ \quad (2)$$

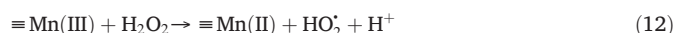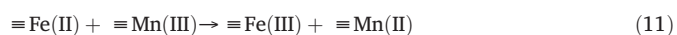$$Fe^{3+} + HO_2^\bullet \rightarrow Fe^{2+} + O_2 + H^+ \quad (3)$$

The important results for the Fenton oxidation for the AHs are given in the supporting information (Table S2). Singa et al. found that the Fenton process was effective in the removal of a mixture of 16 PAHs (92 % removal) under natural pH conditions (Singa et al., 2021). The most popular approach for the controlled release of Fe^{2+} into the treated solution to avoid sludge formation is based on the application of heterogeneous catalysts or modified materials containing Fe. Fard et al. studied the possibility of using nanoscale zerovalent iron (nZVI) as a controlled source of Fe^{2+} in a

Fenton-based reaction for the degradation of BTEX (Alizadeh Fard et al., 2013b). The nZVI undergoes the following reaction in the presence of H_2O_2 (Eqs. (4)–(8)) to form the ROS.

$$Fe^0 + 2 H^+ \rightarrow Fe^{2+} + H_2 \quad (4)$$

$$Fe^0 + H_2O_2 \rightarrow Fe^{2+} + OH^- \quad (5)$$

$$Fe^{2+} + H_2O_2 \rightarrow Fe^{3+} + OH^- + HO^\bullet \quad (6)$$

$$2Fe^{3+} + Fe^0 \rightarrow 3 Fe^{2+} \quad (7)$$

$$Fe^{3+} + 2HO^\bullet \rightarrow Fe^{2+} + H^+ + HO_2^\bullet \quad (8)$$

nZVI-H_2O_2 system caused 99 % of BTEX removal along with an appreciable removal of phenol in 30 min under acidic pH in the presence of UV light (Alizadeh Fard et al., 2013b). Hussain et al. used Fe-based and Zn-based materials as metal activators in Fenton reagents for the removal of pyrene (PYR) and fluoranthene (FLR) from soil matrix and found the prominent effect of Zn (Hussain et al., 2017). Nearly 99 % of PYR were removed by the Zn-based Fenton reagent (under UV light) in 0.5–2 h. In the case of Zn based agent, the Zn reacts with H_2O_2 to form ZnO, an important photocatalyst. Under light irradiation, ZnO generates ROS such as •OH and superoxide radicals ($O_2^{\bullet-}$) for the rapid removal of these PAHs. Li et al. studied the degradation of naphthalene using Fe-Mn binary oxides modified biochar (FeMn/biochar) (Li et al., 2019). Nearly 76 % of the naphthalene was degraded FeMn/biochar – H_2O_2 Fenton system with a major contribution from hydroxyl radicals. The $O_2^{\bullet-}$ played a minor role in the degradation of naphthalene. The biochar played an important role in the adsorption of NAP, further enhancing the oxidation by the ROS generated by the following reactions (Eqs. (9)–(12). The Fe (II)/Fe (III) and Mn (II)/Mn (III) redox cycle favors the oxidation of H_2O_2 and enhances ROS generation.

$$\equiv Fe(II) + H_2O_2 \rightarrow \equiv Fe(III) + HO^\bullet \quad (9)$$

$$\equiv Mn(II) + H_2O_2 \rightarrow \equiv Mn(III) + HO^\bullet \quad (10)$$

$$\equiv Fe(II) + \equiv Mn(III) \rightarrow \equiv Fe(III) + \equiv Mn(II) \quad (11)$$

$$\equiv Mn(III) + H_2O_2 \rightarrow \equiv Mn(II) + HO_2^\bullet + H^+ \quad (12)$$

Mesoporous magnetite/carboxylate-rich carbon (MMCRC) composite as a heterogeneous Fenton reagent has also been tested for the remediation of PAHs in combination with H_2O_2 (Luo et al., 2018). As a photocatalytic material, MMCRC generated reactive species such as $CO_2^{\bullet-}$ and $O_2^{\bullet-}$ under light irradiation. The Fe(II) released by the ligand to metal charge transfer (LMCT) reaction of MMCRC, reacts with H_2O_2 to form •OH. The cumulative reaction of all the reactive species resulted in >90 % removal of phenanthrene from the soil matrix. Lin et al. compared the removal efficiencies of 16 PAHs, using Fenton and a hybrid process with sonolysis from textile dyeing sludge (Lin et al., 2016). Sonofenton treatment resulted in the removal of 73 % of PAHs. The sonochemical production of H_2O_2 (the mechanism is explained in Section 2.5) acts as an indirect source of oxidant in the medium. It could react with the Fe^{2+} controllably to generate ROS. In such a hybrid process, the PAHs adsorbed on the surface of organic matters present in the sludge matrix would be moved towards the interface region of the cavitating bubbles and enhance the degradation efficiency. Dias et al. studied the solar Fenton degradation process of Fluorene based on Fe^{2+} and ferrioxalate complexes (Dias et al., 2018). In comparison with conventional Fenton processes, the ferrioxalate complex is effective under mild pH conditions. In addition, inorganic chelates like sodium pyrophosphate (SP) are employed in the Fenton removal of PAHs such as phenanthrene (PHE) and fluoranthene (FLR). This modified process provided 90 % removal of target PAH.

In recent research, H_2O_2 is replaced by other stable oxidants in Fenton-based reactions. Sodium percarbonate (SPC) and calcium peroxide (CaO_2) are solid materials, which can generate H_2O_2 *in status nascendi* in the treated solution. The advantage of these alternative oxidants is their suitability in a wide pH range and stability. Therefore, SPC-based degradation of organics is now so popular to study. Yang et al. have compared the effectiveness of various oxidants such as H_2O_2, percarbonate, and CaO_2 in combination with Fe^{2+} as Fenton reagents for the degradation of naphthalene (Yang et al., 2021). It has been found that the combination of Fe^{2+} and H_2O_2 is the prime agent for the removal followed by percarbonate. Fe(III) and Fe^{2+} activated SPC have been tested for the removal of benzene and 100 % removal were reported in 1 h through the formation of •OH and O_2•⁻ as the key radical species (Fu et al., 2015; Fu et al., 2017). Xue et al. investigated the possibility to use CaO_2 as an oxidant in the Fenton reaction for the removal of BTEX (Xue et al., 2018). Nearly complete removal of BTEX was also reported using this Fenton system with an oxidant dose of 40/40/1 (CaO_2/Fe(II)/BTEX). When the chelating agents such as citric acid (CA), oxalic acid (OA), and, glutamic acid (GA) are added into the system, the ratio of the oxidants could be reduced to 10/10/1 in the groundwater matrix as well. Likewise, the EDDS–Fe(III)-SPC system enhanced the degradation of Ethylbenzene through the generation of •OH and O_2•⁻ (Cui et al., 2017a). Peroxone, a mixture of H_2O_2 and O_3 in the presence of iron sulfide abundantly generated reactive radical species to decompose benzene resulting in complete mineralization (Hara, 2017). Furthermore, the Fenton process in combination with the biological process enhanced the removal efficiency. Singa et al. studied the removal of Pyr from wastewater using hybrid processes and 85 % removal was reported, which is far better than the individual processes. This hybrid process is efficient and cost-effective (Singa et al., 2021).

Overall, it can be stated that both homogeneous and heterogeneous catalytic processes allow to effectively degrade the AHs. Among the heterogeneous catalysts, nZVI is well suited for the removal (99 % in 20 min), because of the controllable Fe leaching. Alternative oxidants such as SPC, and CaO_2 were also tested in the Fenton system and they can be used as future oxidants. In all the Fenton processes, the concentration of Fe^{2+}/other catalysts (nZVI) and H_2O_2 should be optimized to avoid the excess disposal of oxidants. The chelating agents are capable of reducing the Fe/H_2O_2 concentration in most of the cases to four times.

2.3. Photocatalysis

Photocatalysis is another efficient method reported for water purification. The key mechanism is the generation of electron-hole pair on the catalytic surface by the irradiation of light (Fig. 4). The hole in the valance band oxidises the water molecule to form hydroxyl radical and the reduction of oxygen by the electrons leads to the superoxide radicals (Banerjee et al., 2014; Byrne et al., 2018). Thus, several reactive species are generated in the photocatalytic reactions as given in the following Eqs. (13)–(15). The pollutants could be degraded by any of the ROS based on the nature of the pollutants. The reactivity and the ROS generation are also depending on the catalyst used in the process.

$$TiO_2 + h\nu \rightarrow h_{VB}^+ + e_{CB}^- \tag{13}$$

$$h_{VB}^+ + (H_2O)_{ads} \rightarrow HO^\bullet \tag{14}$$

$$e_{CB}^- + O_2 \rightarrow O_2^{\bullet-} \tag{15}$$

The photocatalytic degradation including the TiO_2-based materials was widely employed for the photocatalytic destruction of AHs from both soil and water matrix (Table 1). According to Len et al. the benzene undergoes adsorption on the surface of TiO_2 surface followed by oxidation (Lin et al., 2020). They found that the intermediate products (acetate, formate, phenol, etc.) affected the adsorption on the catalytic surface and reduce the removal efficiency. Fard et al. studied the photocatalytic removal of BTEX using TiO_2 coated on glass beads (Alizadeh Fard et al., 2013a). This process led to the removal of 92 % of BTEX in just 30 min. The addition of H_2O_2 in the photocatalytic system enhanced the degradation to 99 % and total organic carbon removal to 90 % at neutral pH. In general, the oxidant acts as an electron acceptor to reduce the e-h recombination reaction (Eq. (16)). Also, the H_2O_2 cause the UV photolysis reaction (Eq. (17)). All these make the reaction medium enriched with reactive species. Another merit of combining H_2O_2 is the formation of intermediates. Phenol is the major intermediate product formed during the oxidation of BTEX. The addition of H_2O_2 also fastens the degradation of phenol along with the parent compound. Fernandes et al. found that the photocatalytic processes using TiO_2 in combination with peroxone (O_3/H_2O_2) were effective in the rapid
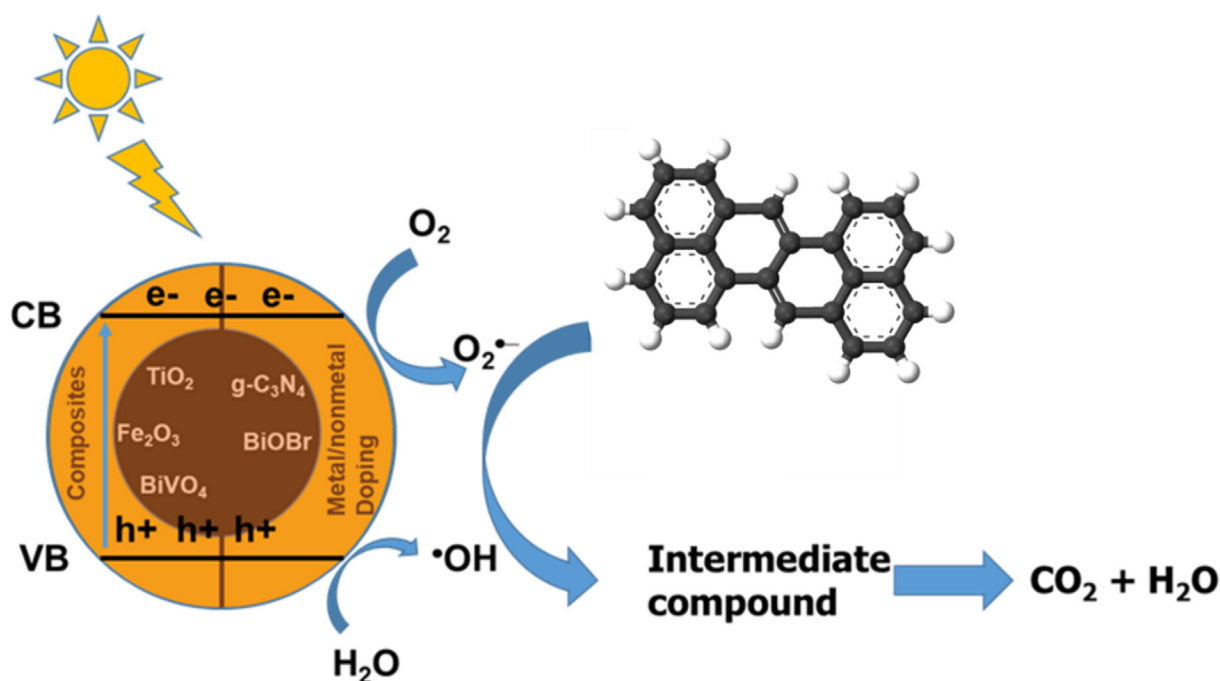

Fig. 4. Various materials used in photocatalysis and their modification for the degradation of PAHs.

Table 1

Photocatalytic-based AOPs approaches for degradation of AHs.

AHs	Experimental condition	% Removal or rate constant	Photocatalyst/UV or visible	Ref.
PHE	[Catalyst] = 1 g/L [PHE] = 200 µg/L Time 12 h	98.6 %	Cobalt-deposited titanate nanotubes (Co-TNT)/simulated solar light	(Zhao et al., 2016)
BaP, BbF, BghiP, BkF, FLR, InD	[Catalyst] = 150 mg/L [PS] = 150 mg/L [PHE] = 850 ng/g Time 8 h	>90 % removal using ZnO	TiO_2, and ZnO/natural sunlight	(Vela et al., 2012)
ANT	[ANT] = 23 ppm [Catalyst] = 55.6 mg/L Time 280 min	90 % removal with ZnO emulsion and 87 % removal with NiO emulsion	ZnO and NiO/UV light	(Sliem et al., 2019)
ANQ	[ANQ] = 0.5 ppm [Catalyst] = 200 mg/L Time 240 min	61 % TOC removal	Faceted TiO_2/solar irradiation	(Ye et al., 2019)
ANT, PHE, CHR, FLU, BaP	PAHs: 50 ppm, [Catalyst]: 25 mg/L, neutral pH Time 48 h Matrices: water and soil	(90 %) > PHE (87 %) > FLU (84 %) > CHR (79 %) > BaP (73 %) In soil; ANT (85 %)> phenanthrene (80 %) > FLU (77 %) > NHR (72 %) > BaP (68 %).	Iron hexacyanoferrate/solar Irradiation	(Shanker et al., 2017)
12 PAHs	[PAHs] = 4,4 µg/g [Catalyst] = 10 % Time: 24 h Matrix: Soil	86–90 %	TiO_2/UVA and UVC	(Eker and Hatipoglu, 2019)
PHE, FLR, and BaP	[PAHs] = 2.0 ppm [Catalyst] = 2.5 % Time: 2 h Matrix: Soil	80 % removal	TiO_2-graphene composite/UV light	(Bai et al., 2017)
CHR	[PAHs] = 2.0 mg/L [Catalyst] = 25 mg Time: 24 h Matrix: water	92 % removal	Fe_2O_3@ZnHCF/sunlight	(Rachna and Shanker, 2018)
2-naphthol	[PAHs] = 100 mg/L [Catalyst] = 0.02 g Time: 1 h Matrix: water	90 % removal	Graphitic carbon nitride/visible light	(Lan et al., 2019)
PHE	[PAHs] = 1 mg/L [Catalyst] = 50 mg/L Time: 6 h Matrix: water	92 % removal	Graphite oxide-TiO_2-Sr $(OH)_2$/$SrCO_3$ nanocomposite/solar irradiation	(Fu et al., 2018)
BAP	[PAHs] = 50 mg/L [Catalyst] = 3 wt% Time: 120 h Matrix: soil	70 % degradation	Iron oxides/UV light	(Gupta and Gupta, 2015)
PYR, PHE	[PAHs] = 50 mg/50 mL [Catalyst] = 50 mg/50 mL Time: 50 min Matrix: water	100 % in 20 min	TiO_2,Fe^{3+}(0.1 %)/TiO_2/visible light	(Theerakarunwong and Phanichphant, 2018)
PHE	[PAHs] = 100 mg/L [Catalyst] = 5 g/L Time: 15 h Matrix: soil	99 % removal	Carbon Xerogel-TiO_2/UV light	(Wang et al., 2020)
PHE	[PAHs] = 200 mg/kg. [Catalyst] = 0.45 g g/15 g Time: 2 h Matrix: soil	84 % removal	g-C_3N_4/Fe_3O_4/visible light	(Wang et al., 2019)
BaANT and BaP	[PAHs] = 2 mg/L [Catalyst] = 25 mg Time: 24 h Matrix: Water	90 % removal	Zinc oxide encapsulated hexacyanoferrate nanocomposite/visible light	(Rachna and Shanker, 2019)
9 PAHs	[PAHs] = 4 × 10^{-4} M [Catalyst] = 0.1 g Time: 8 h Matrix: water	75 % removal	Ag/$BiVO_4$/visible light	(Kohtani et al., 2005)
Benzene	[Benzene] = 460 ppm [Catalyst] = 9 g/L Time: 90 min Matrix: water	100 % removal	Pd/TiO_2/UV-LED	(Selishchev et al., 2021)
BTEX	[Benzene] = 4 mg/L [Catalyst] = 1.5 g [H_2O_2] = 50 mg/L: Time: 30 min Matrix: water	100 % degradation	TiO_2/UV light	(Alizadeh Fard et al., 2013a)

mineralization of volatile organic compounds including BTEX and Naphthalene (Fernandes et al., 2019; Fernandes et al., 2020).

$$e_{CB}^- + H_2O_2 \rightarrow HO^{\bullet} + HO^- \tag{16}$$

$$H_2O_2 + h\nu \rightarrow HO^{\bullet} \tag{17}$$

The photocatalytic degradation of PAHs such as pyrene and phenanthrene has been compared in the presence of a catalyst such as TiO_2, SiO_2, and Al_2O_3 (Wen et al., 2002; Wen et al., 2003). The TiO_2 has shown good removal efficiency over other selected catalysts. Complete degradation and removal of COD were reported by this process. The degradation of PAHs depends on the nature of the compound and as a result, different dosages are prescribed for their degradation. PYR is highly hydrophobic in nature and is stronger adsorbed on the TiO_2 surface than PHE. It undergoes faster degradation at the catalyst surface and likely form hydrophilic intermediate products which are desorbed from the material surface (Dong et al., 2010). Woo et al. also found that TiO_2 is effective in the removal of PAHs such as naphthalene, acenaphthylene, phenanthrene, anthracene, and benzo[a]anthracene (Woo et al., 2009). By-products formed during the process are revealed to also undergo effective degradation. Moreover, the aggregation of the materials generally reduces their photocatalytic activity. In order to prevent the aggregation and enhance the photocatalytic activity several modifications to the catalyst have been reported. Carbon xerogels generally possess a network structure to capture the nanomaterials inside and prevent agglomeration (Wang et al., 2020). It has a large surface area and thus possesses more adsorption sites. These kinds of properties are suitable for the effective degradation of PAHs like pollutants. As result, the material offered 79 % adsorption efficiency and 97 % removal efficiency. Structural modification of TiO_2 has also been done to improve their adsorption capacity. Among them, one-dimensional titanate nanotubes (TNTs) have gained significant attention in pollutant removal owing to their high surface area and are easily separable from the liquid matrix (Liu et al., 2013; Xiong et al., 2011). The applicability of such material was also tested for the removal of PAHs. It is noted that the adsorption of PAHs on these materials is negligible, thus oxidation is the key mechanism responsible for their removal. The sole use of TNTs revealed only 10 % removal of phenanthrene even after 12 h. Doping of Co ion in the TNTs (Co-TNT) at high temperature resulted in a significant improvement in the removal efficiency - 99 % degradation was reported in 12 h - with appreciable reusability (Zhao et al., 2016). Like TiO_2 nanoparticles, the electron-hole recombination rate is high for TNTs. However, in Co-doped TNTs, the electrons are transferred by CoO along with Co^{2+}/Co^+ reduction cycles. The stored electrons react with O_2 to produce superoxide radicals. All these species would then react with the PAHs.

Likewise, the diatomite-supported TiO_2 enhanced the removal of naphthalene under plasma irradiation (Wu et al., 2018). In a plasma-based photocatalytic reaction, the electrons discharged from plasma reactions are able to generate e-h pair. The Ti^{4+} after the plasma irradiations are reduced to Ti^{3+}, which is more susceptible to photocatalytic reactions. However, TiO_2-based methods were employed under UV light irradiation. Therefore, several modifications have been done to TiO_2 and its related composites are developed to be active in the visible light region. Fe doped-TiO_2 has good photocatalytic activity in the visible range and is used for the removal of Phenanthrene, Fluoranthene, and Anthracene (Theerakarunwong and Phanichphant, 2018). This material offered >60 % of the PAHs removal. Solar light active Fe_2O_3/TiO_2 were studied for the degradation of NAP. 91 % of the initial NAP was degraded under solar light irradiation. This was further enhanced by the addition of PMS. In this case, the additional of reactive species, $SO_4^{\bullet-}$ were formed by the reaction of the photogenerated electron with PMS (Sayed et al., 2022). Pd doped on TiO_2 was effective in the complete removal of benzene in 240 min (Selishchev et al., 2021).

TiO_2 immobilized on activated carbon is an emerging catalyst for the photocatalytic oxidation of pollutants. The advantage of including an adsorbent is to fasten the oxidation reaction on the surface of the catalyst. This material has shown excellent photocatalytic properties for the removal of Naphthalene (Zeng et al., 2021b). The incorporation of a composite activator mixture of Fe^{3+} and Zn^{2+} further enhanced the removal efficiency to 75 %. Along with activated carbon, Zn^{2+} increases the possible adsorption sites for PAHs. The Fe^{3+} enhanced the visible light activity of the material. In the same way, TiO_2-graphene nanocomposites applied for the removal of PAHs such as Phenanthrene (PHE), fluoranthene (FLAN), and benzo[a] pyrene (BaP) (Bai et al., 2017). This material has shown excellent adsorption for the PAHs and nearly 80 % of the removal was reported in 180 min. Another advantage of incorporating the graphene composite is its ability of charge transportation reactions. In order to further improve the photocatalytic reactions of the above composites, strontium ion is decorated on the surface. This material has shown 90 % removal of phenanthrene in 350 min, which is two times better than the individual materials.

In addition, many visible light active catalysts such as Bismuth oxybromide (BiOBr) and Bismuth vanadate ($BiVO_4$) are widely applied for photocatalytic applications (Arumugam et al., 2021). Bi^{3+}-containing catalysts are characterized by high visible light activity and have lower bandgap energy due to the presence of O 2p and Bi $6s^2$ hybridized valence band. An important advantage of BiOBr is its unique layered structure, which is stable and non-toxic. All these advantages have taken for various photocatalytic applications mostly in the removal of different kinds of organic contaminants. However, the lower band gap energy of BiOBr causes the faster electron-hole recombination reaction. Therefore, several modifications such as doping, and the preparation of composites with other semiconductor oxides lessen the recombination possibilities (Monfort and Plesch, 2018). These kinds of modified materials were utilized in the removal of PAHs. In the case of TiO_2/BiOBr nanocomposite, it was confirmed that obtained treatment effect was obtained by generated ROS such as •OH, and $O_2^{\bullet-}$ formed under visible light irradiation providing effective degradation of anthracene. The composite offered a better removal of anthracene compared to the individual materials such as TiO_2 or BiOBr (Sun et al., 2021). Kohtani et al. studied the removal of PAHs using $BiVO_4$ photocatalyst under visible light irradiation. They have compared the efficiency of doped (with Ag) and non-doped $BiVO_4$ for the conversion of PAHs. The oxidation rate of PAHs using Ag-doped $BiVO_4$ was faster than that of the non-doped material. It was also clear in the formation of one of the oxidation products, anthrone during oxidation. Like other mechanisms involved in doping, the incorporation of Ag enhanced the light absorption and electron-hole separation (Kohtani et al., 2005).

Graphitic carbon nitride (g-C_3N_4) is an emerging metal-free photocatalyst composed of carbon and nitrogen. Since it is stable under a wide temperature range and in various solvents, g-C_3N_4 has been used for a variety of environmental applications. It has shown its role in the removal of pollutants both by adsorption and oxidation. Like other photocatalysts, modified g-C_3N_4 was also available to improve the removal efficiency (Ong et al., 2016; Sudhaik et al., 2018). In contrast to other photocatalyst, the N vacancy makes it strong adsorbent and more photoactive. The degradation studies of phenanthrene in the soil matrix using g-C_3N_4 were reported and 40 % of the PAHs were removed. Moreover, the composite of g-C_3N_4 with Fe_3O_4 enhanced the degradation percentage to 90 % (Wang et al., 2019). As described previously, the iron oxide layer acts as an electron storage center and generates more $O_2^{\bullet-}$ species. In the same way, a ZnO/g-C_3N_4 heterojunction material was fabricated for the degradation of NAP under visible light irradiation. More than 84 % of NAP was degraded in 4 h using this photocatalyst (N. Mukwevho et al., 2019). Visible light active Ag/Ag_3PO_4/g-C_3N_4 heterojunction nanocomposite was utilized for the degradation of phenanthrene. In this nanocomposite, the g-C_3N_4 is covered on the surface of Ag_3PO_4 and the Ag acted as the charge transfer bridge between them. The presence of Ag enhanced the visible light absorption capacity of the material. The reported degradation of PHE under visible light irradiation using this material was 90 %, which is 4 times higher than that of the individual material (Dai et al., 2022).

Iron oxides are another important material for the photocatalytic degradation of PAHs (Gupta and Gupta, 2015). In comparison with the other semiconductor metal oxides, these materials are available in nature in mineral form. Goethite (α-FeOOH), hematite (α-Fe_2O_3), lepidocrocite (γ-

FeOOH), and maghemite (γ-Fe$_2$O$_3$) are the major Fe minerals found in nature and used in the removal of pollutants. Thus, they can easily be implemented in soil remediation as well. The inclusion of iron oxides (especially, α-FeOOH) in the pyrene contaminated site resulted in 70 % removal after 120 h of contact time. The removal rate by iron oxide materials is dependent on the light intensity and catalyst dosage. Furthermore, the addition of ligands enhanced the photochemical production of reactive species in the iron oxide system. As an example, the addition of oxalic acid in the iron oxide system resulted in the complete removal of pyrene. Oxalic acid generates the Fe-oxalate complex in the solution and has good light absorptivity. This complex also induces a Fenton-type reaction to enhance the oxidation reaction. In this way, all the dissolved iron species could be utilized for the reaction. This kind of ligand-mediated photoreaction of the Fe^{3+}-smectite complex was reported for the removal of phenanthrene (Jia et al., 2015). The ligands such as oxalic acid, citric acid, EDTA, and nitrilotriacetic acid were used. The Fe^{3+}-smectite has resulted in the 90 % conversion of phenanthrene under visible light. Among these ligands, oxalic and malic acid showed the complete degradation of the target pollutant in 6 h. The Fe^{2+} formation and the nature of Fe-ligand are important factors in this kind of reaction.

Metal hexacyanoferrates especially, Iron and Zinc hexacyanoferrates (FeHCF and ZHCF) are used in environmental remediation owing to the semiconductor properties and large surface area (Rachna and Shanker, 2019). From the environmental point of view, these materials are stable, non-toxic, and don't undergo degradation in the natural environment. Thus, it can be used for the long-time treatment in the contaminated site. The lower band gap (1.3–2.5 eV) makes it to accessible in the visible region. This material offered 90 % removal of PAHs (Anthracene, phenanthrene, Fluorene, chrysene, and Benzo[a]pyrene) under neutral pH conditions in 48 h. Moreover, the ZnO encapsulated FHCF has been developed for the removal of PAHs, which are reactive under sunlight (Rachna and Shanker, 2019). In the same way, Fe$_2$O$_3$ doped on ZHCF has been used for the removal of chrysene (Rachna and Shanker, 2018). 90 % of the chrysene removal was reported using this catalyst after 24 h under sunlight irradiation. The advantage of the material is its effectiveness in a wide range of pH and is effective even after ten consecutive cycles. Further, many efforts have been done to develop improved visible light active materials for the degradation of PAHs. Because of the defective-rich ultrathin layered structure, BiO$_{2-x}$ has been used as a visible and NIR light-responsive photocatalyst. A ternary composite of BiO$_{2-x}$/Ag$_3$PO$_4$/CNT was reported to be effective for the degradation of NAP and PYR (Jin et al., 2020). More than 90 % of the NAP and 80 % of PYR were degraded with the use of this catalyst under visible light irradiation. In this case, the major reactive species were •OH and O$_2$•⁻. The photoirradiation on the surface Ag$_3$PO$_4$ generates metallic silver by the reduction caused by the photogenerated electron migrated. The formed Ag in the interface of the composite can generate more electrons by the localized surface plasmon resonance effect. The photogenerated hole would then transfer to VB of BiO$_{2-x}$. As a result, abundant e-h pairs are formed on the surface of the composite and finally on the surface of CNT. The CNT favors the adsorption of PAHs and significantly improves oxidation. Similarly, a composite of Ag$_3$PO$_4$ and graphene oxide sheet, KOH-modified biochar and g-C$_3$N$_4$, Mn$_3$O$_4$/MnO$_2$-Ag$_3$PO$_4$, revealed excellent performance in the visible light region for the removal of PAHs (Cai et al., 2019; Lin et al., 2022; Yang et al., 2018). All the composites were effective in reducing the electron-hole recombination reactions (Nguyen et al., 2020).

Reviewed material in this part reveals that photocatalytic materials such as TiO$_2$, and ZnO are employed in the effective degradation of AHs. However, these materials are active only in the UV region. Several composite materials were proposed to improve the adsorption of PAHs on the material surface and metal ions were doped to reduce the e-h recombination reactions. The materials such as g-C$_3$N$_4$, Ag$_3$PO$_4$, BiVO$_4$, BiOBr, and their composites were used in the photocatalytic degradation in the visible light region revealing effective AHs degradation. Fe or Co doping is preferred in most of the photocatalytic systems because of the electron storing capacity of the material. The combination of catalysts with oxidants such as H$_2$O$_2$ and PS resulted in the complete degradation of AHs within a short period.

2.4. Sonochemical degradation of AHs

Ultrasound-based AOPs are the emerging technique widely used for the removal of organic contaminants. The ultrasound induces the vibration of intermolecular motion once it passes through the liquid medium. It results in the generation of microbubbles during the acoustic cycles. The size of the bubbles gets increased in the subsequent compression and rarefaction cycle and undergoes implosion after reaching its critical size (Fig. 5A). The temperature and pressure are increased up to 5000 K and 500 atm pressure adiabatically as a result of bubble collapse (Gągol et al., 2018a; Gągol et al., 2018b; Rayaroth et al., 2016). This extreme condition is sufficient for the pyrolytic cleavage of a water molecule to •H and •OH (Fig. 5A and B). Further reactions lead to different radical species in the medium to form a variety of ROS as given in Eqs. (18)–(22).
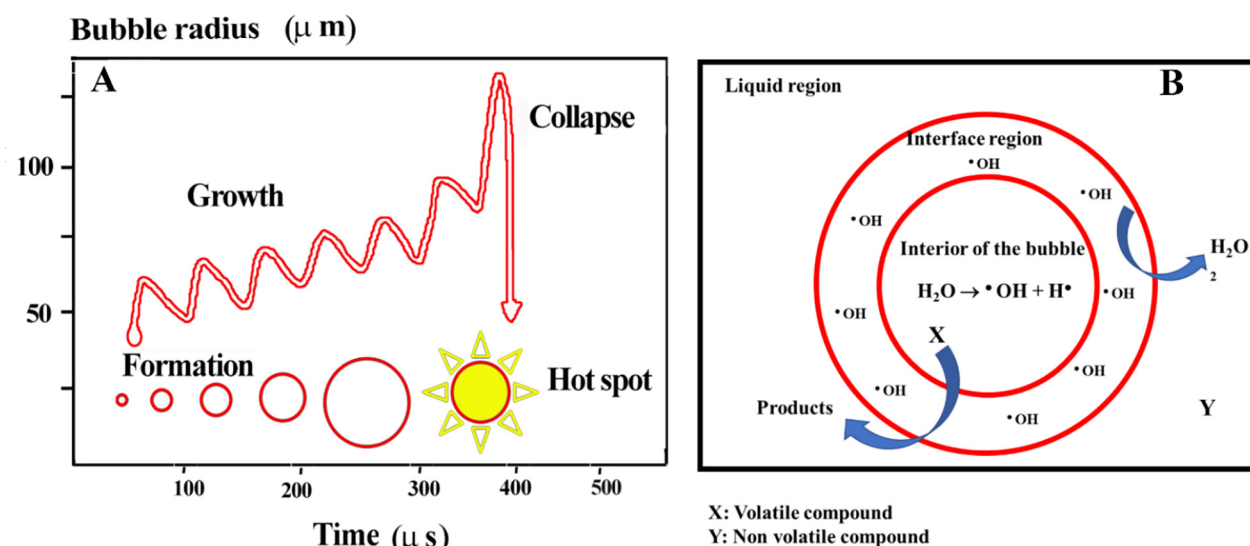
$$H_2O \text{))) } \rightarrow HO^\bullet + H^\bullet \tag{18}$$

Fig. 5. The cavitation processes (A) and the various reaction zones (B) in cavitation-based AOPs (Rayaroth et al., 2016).

$$HO^\bullet + H^\bullet \rightarrow H_2O \tag{19}$$

$$2HO^\bullet \rightarrow H_2O_2 \tag{20}$$

$$2H^\bullet \rightarrow H_2 \tag{21}$$

$$H^\bullet + O_2 \rightarrow HO_2^\bullet \tag{22}$$

Moreover, there are many other reaction possibilities as the reactive cavitating bubbles are considered. The cavitating bubbles are considered a hot spot region and it consists of three reactive zones (Fig. 5B). The interior of the bubble is the high-temperature region and is highly susceptible to the thermal reactions. Volatile compounds undergo fast degradation in this region. The bubble-liquid interface region is hydrophobic and hydrophobic pollutants would drag into this region to undergo degradation by the radical attack and by pyrolysis. The hydrophilic compounds usually remain in the liquid region and their degradation is slow in sonolysis, because only radical reaction is possible. Briefly, the degradation of pollutants is strongly dependent on their ability to move in any of these three reactive zones. PAHs are hydrophobic in nature and therefore their degradation occurs mainly in the interface region of the cavitating bubble.

The efficiency of the cavitation process in the degradation of AHs is given in the supporting information (Table S3). Nearly 99 % degradation of phenanthrene was reported by the application of 582 kHz frequency ultrasounds and power 133 W after 100 min. in the same way, 99 % of the naphthalene was degraded at a frequency of 80 kHz at a power of 150 W. The toxicity of the treated water was decreased significantly ensuring the formation of less toxic byproducts. David et al. also compared the removal of PAHs at two frequencies such as 20 and 506 kHz (David, 2009). In this process, 506 kHz has shown maximum removal. Manariotis et al. also investigated the effect of operational parameters such as frequency, power, and volume on the degradation of PAHs such as phenanthrene, naphthalene, and pyrene (Manariotis et al., 2011). Among the three frequencies such as 582 kHz, 862 kHz, and 1142 kHz, the 582 kHz resulted in the highest removal of PAHs (90 % for naphthalene, 100 % for phenanthrene, and 99 % for pyrene). The size of the bubbles was estimated by a laser diffraction study, doppler method, and sonoluminescence method (Burdin et al., 1999; Iida et al., 2010; Lee et al., 2005). The study revealed that an increase in frequency from 515 kHz to 1100 kHz led to a decrease in bubble size from 2.8 to 3.7 μm to 0.9–1.38 μm. The estimated bubble size was 3.9, 3.2, 2.9, 2.7, and 2.0 μm respectively for the frequencies at 213, 355, 647, 875, 1056, and 1136 kHz and power at 3 W. Manariotis et al. correlated the role of bubble size in the degradation of PAHs (Manariotis et al., 2011). The bubble radius calculated at the frequencies 582 kHz, 862 kHz, and 1142 kHz were 5.1 μm, 3.5 μm, and 2.6 μm and the number of bubbles calculated was 8.1×10^9 number/L, 3.7×10^{10} number /L, and 1.2×10^{11} number /L. The large-sized bubbles formed at a lower frequency increase the possibility of recombination reactions of free radicals at the interface region. This factor limits their diffusion into the liquid region or their possible reaction with PAHs.

However, an increase in power increases the number and size of the bubbles in the medium. As reported by Sunartio et al. an increase in bubble size from 1.9 to 4.5 μm was observed by increasing the applied power from 2 to 10 W (Sunartio et al., 2005). Furthermore, the cavitating bubbles undergo intense collapse at high power, which caused a high temperature and a higher abundance of reactive species. Surprisingly, the lower molecular weight PAHs have shown different behavior in sonolysis under varying power. At the high ultrasonic power intensities of 51.75 W/cm² power releases a large number of •OH into the medium and completion occurs between these two categories of PAHs. Gągol et al. studied the cavitation process for the removal of BTEX from an aqueous medium, and 55 % removal was reported using acoustic cavitation processes. In addition, when it is combined with oxidants like H_2O_2, O_3, and peroxone ($O_3 + H_2O_2$), the removal efficiency increased to 100 % in 60 min. A similar effect was shown in the case of the hydrodynamic cavitation process, where the effect of oxidants was even more visible (Gągol et al., 2018b).

Sponza et al. reported the removal of PAHs (benzo[*a*]pyrene (BaP), benzo[*k*]fluoranthene (BkF), acenaphthylene (ACL), and carbazole (CRB)]) at a frequency of 35 kHz (Sponza and Oztekin, 2011). Nearly 80 % of the PAHs were removed after 150 min of sonication. The CCl_4, as an additive in sonolysis, enhanced the removal efficiency to 97 % due to the evolution of additional reactive chlorine species as given in Eqs. (23)–(26).

$$CCl_4 + H^\bullet \rightarrow H^+ + Cl^- + {}^\bullet CCl_3 \tag{23}$$

$$Cl^- + Cl_2 \rightarrow Cl_3^- \tag{24}$$

$$Cl_3^- + H^\bullet \rightarrow H^+ + Cl_2^\bullet + Cl^- \tag{25}$$

$$H_2O_2 + HClO \rightarrow Cl^- + H_2O \tag{26}$$

This study compared the removal of less hydrophobic (acenaphthylene (ACL) and carbazole (CRB)) and more hydrophobic PAHs (benzo[*a*]pyrene (BaP) and benzo[*k*]fluoranthene (BkF)) at different pHs. The removal rate of the first category of PAHs was reported to be higher at alkaline pH, while for the second category of pollutants, acidic pH favors higher removal. Protonation of the more hydrophobic PAHs further increased their hydrophobicity and tend their accumulation in the hydrophobic region of the cavitating bubbles and cause higher removal by radical reaction and pyrolysis. Acidic pH results in the formation of positively charged bubbles due to the accumulation of hydronium ions in the interface region. Therefore, this may increase the number of bubbles in the medium without undergoing bubble coalescence. Thus, the recombination rate of •OH in the interface region is less occurring under acidic pH. This condition increases the number of ROS available in the interface region of the cavitating bubble and the solution region for degradation. The increase of alkalinity of less hydrophobic PAHs increases the solubility and hydrophilicity of the PAHs. This compound is more susceptible to degradation by •OH. Thus, the ionization of these PAHs causes their presence in the liquid region of the cavitating bubbles where more •OH radicals are accumulated. Moreover, the changes in the pH affect the PAH degradation in presence of CCl_4 as well. This is due to the competition for the interface region of the cavitating bubbles for PAHs and CCl_4. In addition, the occurrence of reactive chlorine species was pH-dependent. Acidic pH favors the hypochlorous acid (oxidation potential 1.49 V) whereas the alkaline pH yields hypochlorite (0.94 V) during the sonolysis of CCl_4. Furthermore, the salting-out effect enhanced the degradation of PAHs in sonolysis. Sponza et al. further reported that persulfate ions enhanced the degradation through the generation of sulfate radicals (Sponza and Oztekin, 2010). Sonolysis in combination with Fenton was also effective in the removal of PAHs even from the complex matrices (Ke et al., 2018). Lin et al. further confirmed that these hybrid processes are more effective in textile dyeing sludge matrix than their process (Lin et al., 2016). The sonication releases the adsorbed PAHs from the sludge matrix due to the physical effect and the oxidation capable of removing the chemicals from the water medium. A similar effect is reported in nZVI/EDTA/Air (ZEA) system under ultrasound irradiation (Lai et al., 2019). The combined system is more effective (70 % degradation) than individual processes such as ZEA (42.5 %) and US (33 %) for the removal of a mixture of 16 PAHs. ZEA system generates the ROS by the following mechanism and Fe(IV) species (through the reaction Fe^{2+} and in situ formed H_2O_2). In general, the two-electron oxidation of O_2 by Fe^0 generates H_2O_2 in the medium. The Fe^{2+} released from the corrosion of Fe^0 induces the Fenton reaction with the as-generated H_2O_2 to form ROS (Fig. 6). In the presence of US, the concentration of H_2O_2 in the medium got increased, which may increase the effectiveness of the Fenton reaction. In the sludge matrix, the sonication helps to desorb the PAHs from the sludge into the solution phase. Further, they can be degraded by oxidation.

In short, the cavitation-based AOPs showed advantages over other processes for the AHs degradation. Since the AHs, and especially the PAHs, are highly hydrophobic, their degradation seems to be more prominent in the liquid-gas interface region of the cavitating bubble. However, the inclusion of reagents like PS, H_2O_2, and CCl_4 increased the availability of reactive
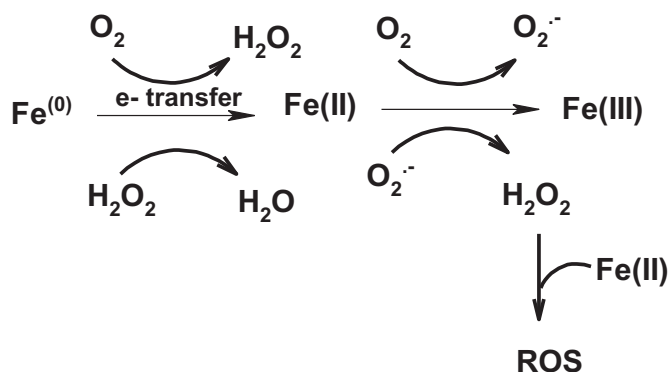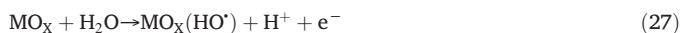
Fig. 6. Generation of ROS in ZVI-air system.

species in the liquid region, which is more suitable for hydrophilic AHs (derivatives of unsubstituted AHs).

2.5. EAOPs for PAHs

Electrochemical advanced oxidation processes are one of the versatile techniques in AOPs due to their effective generation of reactive species and various reaction possibilities (Brillas et al., 2009; Sirés et al., 2014). On the electrodes, the pollutants can undergo direct oxidation by the exchange of electrons between the pollutants and the electrode surface. It can be represented by (27)–(28).

$$MO_X + H_2O \rightarrow MO_X(HO^\bullet) + H^+ + e^- \tag{27}$$

$$MO_X(HO^\bullet) + PAHs \rightarrow\rightarrow mineralisation \tag{28}$$

where, MO_x is the representative electrode.

Another reaction induced by the applied potential difference is the generation of H_2O_2 by the two-electron oxidation at the cathode surface (Eqs. (29)–(30)).

$$O_2(g) + 2H^+ + 2e^- \rightarrow H_2O_2 \tag{29}$$

$$O_2(g) + 4H^+ + 4e^- \rightarrow 2H_2O \tag{30}$$

The above-generated H_2O_2 would undergo a Fenton-type reaction with the added Fe^{2+} to amplify the ROS generation, called the electro Fenton process. Both direct oxidation and Fenton processes were applied for the removal of a variety of organic pollutants including PAHs (Fig. 7). The efficiency of EAOPs further depends on the electrode materials, electrolytes, salt, reaction temperature, etc. In many cases, the EAOPs are implemented for large-scale wastewater treatment systems, toilet water treatment systems, etc.

PAHs undergo an initial electron transfer reaction at the electrode surface to form a radical cation of PAHs, which undergoes further degradation. Moreover, in the solution phase, it undergoes Fenton oxidation like other AOPs. There are various electrodes Ti/RuO$_2$, Ti/IrO$_2$, Ti/TiO$_2$, Ti/SnO$_2$, Ti/SnO$_2$–Sb$_2$O$_5$–IrO$_2$, Ti/Sb-SnO$_2$/PbO$_2$, Ti/SnO$_2$-Sb$_2$O$_5$-RuO$_2$, etc. tested for the PAHs removal in EAOPs (Ajab et al., 2020; Rajasekhar et al., 2021; Tran et al., 2009; Yaqub et al., 2015). The degradation of BTEX was reported using a CNT-Ce/WO$_3$/GF electrode and 60 % of COD was reduced in 90 min. Yaqub et al. studied the removal of 16 PAHs using Ti/SnO$_2$ electrodes, and 80 % of the total PAHs were removed (Yaqub et al., 2015). The electrode Ti/RuO$_2$ offered 93 % and 82 % removal of PAHs in aqueous and creosote solution respectively using Na$_2$SO$_4$ as the supporting electrolyte in 90 min (Tran et al., 2009). The removal efficiency increased with an increase in the Ru content in the anode. In the same way, the electrolysis using Ti/SnO$_2$-Sb$_2$O$_5$-RuO$_2$ electrode resulted in 93 % removal of PAHs after 3.9 h (Yaqub et al., 2015). Even though the EAOPs are effective in the degradation of AHs, there are not many studies reported utilising this technique. The electrodes used in this case are Ti/SnO$_2$–Sb$_2$O$_5$–IrO$_2$, Ti/Sb-SnO$_2$/PbO$_2$, Ti/SnO$_2$-Sb$_2$O$_5$-RuO$_2$, etc. Many oxidants such as H$_2$O$_2$, PS, HOCl, etc., can also be combined in the electrochemical system to get better performance.
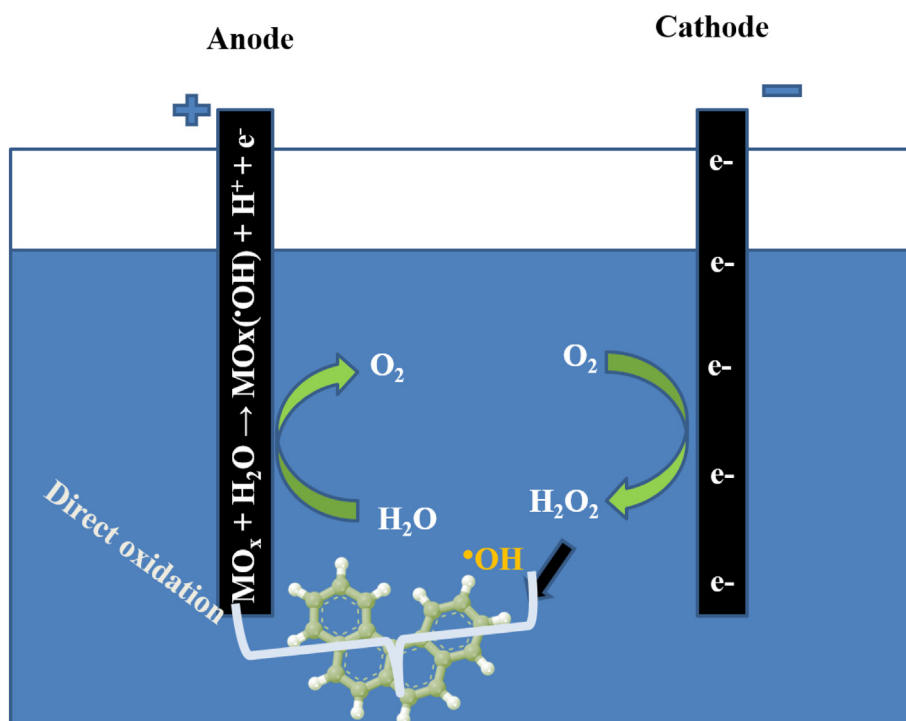
Fig. 7. Schematic representation for the generation of various degradation pathways involved in EAOP.

2.6. Sulfate radical based AOPs (SR-AOPs) for PAHs

Persulfate (PS) is an emerging chemical oxidant as it possesses a high redox potential of 2.01 V. In comparison with other oxidants, it is stable, has a wide application range of pH, is water-soluble, and more easily enters into the contaminated site of lower permeability zone. The ROS generated are •OH, $SO_4^{•-}$ and $^1O_2$ responsible for the oxidation of organic pollutants. Peroxydisulfate (PDS, $S_2O_8^{2-}$) and peroxymonosulfate (PMS, HSO_5^-) are the commonly used oxidants in PS-based AOPs. Among them, PDS is more cost-effective and hence used in environmental applications including the in situ chemical oxidation processes (Zhang et al., 2015; Zhou et al., 2019).

PDS is generally applied for the removal of BTEX and PAHs from soil matrices since the PDS in the soil matrix could be activated by the minerals, soil organics, and biologically active substances (Table S4). The injection of PDS to BTEX contaminated site resulted in 92 % degradation in 3 weeks and for PAHs meanwhile, it takes more than a month to reach 95 % degradation (Liang et al., 2008; Xu et al., 2021). This is rather a slow rate and the major degradation product observed was hydroxyl-PAHs, which are also degraded with time. An important advantage of this method is the possibility to couple it with biological remediation processes. A binary system of H_2O_2-PDS was also reported as an effective method for the removal of PAHs, where nearly 90 % removal was achieved (Zhao et al., 2013). Another dual oxidant system, PMS-KMnO₄, revealed an excellent degradation capability towards benzene. The combined system was much more efficient compared to the individual oxidants. The advantage of this system is that it can generate MnO_2 in situ, which can further activate and oxidize the contaminants (Cui et al., 2017b).

$$PDS/PMS + activators \rightarrow SO_4^{•-} \tag{31}$$

Furthermore, to get a faster reaction of PDS/PMS, appropriate activators were included (Eq. (31)). Such activators for soil remediation are iron-based materials, heat activation, base activation, and electrochemical activation. While, for the aqueous phase removal, UV, ultrasound, and heterogeneous catalysts have been reported. Fe-based materials are found as effective materials for the cleavage of peroxobond of the PS. The activation thus generates the ROS in the medium. The various activated PS method reported for AHs are given in Table S4.

As an example, the Fe^{2+}-PDS system was successful in the removal of pyrene in water and soil. Nearly 93 % and 88 % of the pyrene were degraded from water and soil respectively (Guo et al., 2021). In the case of BTEX, 80 % was removed in just 7 min. However, in the Fe^{2+}/PDS system, the iron precipitation makes the processes less efficient in real field applications like for other Fenton-based processes. Therefore, many methods were adapted to minimize iron precipitation. Chelation is one of the common methods in this aspect, where the iron hydroxides are chelated to a more soluble form and activate the oxidants. Citric acid (CA) is one of the widely studied chelates in this process. Zeng et al. have investigated the removal of naphthalene using the Fe^{2+}-PDS system with chelation using CA (Zeng et al., 2021a). The sole Fe^{2+}/PDS system caused the degradation of 50 %, the efficiency got increased to 98 % in the presence of CA. In the same way, Fe^{2+} chelated by oxalic acid (OA) activated the dual peroxide system CaO_2/PDS to enhance the removal of a mixture of PAHs (Wang et al., 2021; Yuan et al., 2019). Ligands such as ethylenediaminetetraacetic acid (EDTA), and ethylenediamine-N, N′-disuccinic acid (EDDS) chelated with Fe tested for the removal of naphthalene, where EDTA performed well for the removal from the soil matrix (Yan and Lo, 2013). The chelation enhanced the desorption of PAHs adsorbed on the soil matrix. The electron transfer of the Fe complex to the ligand is the key mechanism in the generation of ROS in this process. The inorganic ligand, SP resulted in nearly 95 % and 92 % of the PHE and FLUT in Fe-activated PDS.

In order to control the Fe release, various heterogeneous catalysts and nZVI-based materials have been developed. Peluffo et al. had compared the removal of PAHs (anthracene (ANT), phenanthrene (PHE), pyrene (PYR), and benzo[a]pyrene (BaP)) by various activators of PS such as Fe^{2+}, Fe^{3+}, and nZVI (Pardo et al., 2016; Peluffo et al., 2016). Among these iron species, nZVI has a prominent effect on PS activation, which resulted in the controlled release of reactive species. A sole PS resulted in nearly 40 % removal of PAHs, and HPAHs. The simultaneous application of heat and nZVI strongly activates the PDS to degrade the PAHs to nearly 90 %. The synergistic activation process enhances ROS generation. nZVI/PMS system was tested for petroleum hydrocarbon removal from the soil matrix. The removal efficiency of >96 % was achieved by this process. Acidic pH and alkaline pH were very suitable for efficient removal (Bajagain and Jeong, 2021). As given in the previous sections, the chelating agents would be an important additive to enhance the removal efficiency in such processes. Zeng et al. combined citric acid with a ZVI/PS system for the degradation of NAP. In this study, they used both PMS and PDS to generate the reactive species. The PMS/nZVI/CA offered removal of 96.5 % and PDS/nZVI/CA resulted in 93.5 % degradation from the soil slurry system. The effect of chelation is already described in the papers on Fenton processes (Zeng et al., 2022).

A magnetic carbon microsphere-based composite catalyst (Fe_3O_4 − CM) and carbon black supported Fe_3O_4 (Fe_3O_4-CB) were able to activate PS for the removal of PAHs from marine sediments (Dong et al., 2019; Dong et al., 2018). Similar material was also tested for the removal of BTEX from an aqueous medium and a practical removal was reported (Dong et al., 2017b). Porous carbons are widely used as catalysts in environmental engineering. The high surface area of the material favored the adsorption of the organic contaminants on their surface and facilitate the oxidation of contaminants. The redox properties of these materials are capable of persulfate activation to generate the reactive oxygen species. The CM in the catalyst acts as an additional site for PDS activation through an electron transfer mechanism. Likewise, iron-based bimetallic nanoparticles (Fe-Ni) supported on activated carbon (AC) activate PDS to generate various ROS and degrade the PAHs. Another carbon-enriched material is biochar. Several studies revealed its usefulness as a PS activator. These materials can very effectively adsorb the PAHs from the contaminated site as well as activate oxidants for PAHs degradation. Metal-free biochar derived from a Green seaweed (*Ulva lactuca*) activated PMS resulted in the degradation of 75 % of PAHs. In this case, the degradation efficiency was decreased with the number of rings in the structure (Hung et al., 2022). The PS activation capacity of biochar and thereby the removal efficiency is increased by N-doping. A 80 % of the PAHs was degraded in the sediment sample when PMS was activated by an N doped Biochar. The process was effective in a wide range of pH (3 − 11). The nitrogen in the biochar acted as an additional site for PMS activation. The charge transfer was facilitated by N, which further enhanced the PMS activation. Singlet oxygen ($^1O_2$) was also generated in addition to other reactive species from the electron shuttling through the C═C of the biochar (Hung et al., 2021). Iron and copper nanoparticles supported on biochar/geopolymer were an effective PMS activator, effective in NAP removal from both aqueous and soil matrix. Like other metals, the redox cycle favored the PMS activation by these species (Zhu et al., 2022).

The Fe_3O_4 immobilized on Biochar removed >80 % of the PAHs (mixture of LPAH and HPAH) from the soil matrix after 25 h (Dong et al., 2017a). The surface modification with metal or non-metal doping enhanced the adsorption and the reactivity of the material (Oh et al., 2019; Zaeni et al., 2020). Moreover, there is a study to control the PS release to increase the life of the oxidation process. Polystyrene-coated persulfate polyacrylonitrile beads (PC-PSPANBs) were synthesized for the controlled release of PDS for the removal of PAHs such as acenaphthene (ACE), 2-methlynaphthalene (2-MN) and an oxygenated PAH, dibenzofuran (DBF) (Abbas et al., 2021). The inclusion of Fe^{2+} in the PDS-controlled system offered the good removal of all the selected PAHs even in the presence of ionic species such as Cl^- and SO_4^{2-}.

Manganese (Mn) based materials are also employed in the removal of organics from contaminated soil (Zhu et al., 2019). Kan et al. studied the effect of Mn oxides on the removal of pyrene using microwave-assisted PDS oxidation by the radical and non-radical process (Kan et al., 2021). Microwave-assisted PDS oxidation degraded 65 % of pyrene from the

matrix in 15 min and the efficiency is increased to 87 % with the introduction of MnO_2. As in the case of the normal PDS oxidation method, the main reactive species involved are $SO_4^{\bullet-}$ and $\bullet OH$. While in the combined process, the $O_2^{\bullet-}$ and $^1O_2$ are the key species. Bai et al. studied the electrochemical activation of PMS for the treatment of 16 PAHs from textile dyeing sludge. The process utilized the electrochemically generated Fe^{2+} for the PMS activation. A sacrificial Fe electrode was used in this case for the effective activation of PMS. Nearly 73 % of the Σ16PAHs were removed using this technique: The electrochemical activation depends on the ability of the Fe anode for the generation of Fe^{2+} and their electrochemical regeneration (Bai et al., 2022).

PDS activation by ultrasound is another method to remove phenanthrene from the contaminated matrix (Deng et al., 2015). The high temperatures occurring by the cavitation process are sufficient for bond cleavage of PDS. The US-activated PDS provided complete degradation of phenanthrene in just 30 min due to an increase of temperature of up to 5000 K. Hydrodynamic cavitation processes were also efficient in the generation of reactive species and >90 % of the BTEX was removed in 240 min of treatment (Fedorov et al., 2021).

A novel PDS and PMS activator, asphaltenes were introduced by Fedorov et al. for the degradation of BTEX (Fedorov et al., 2020). The PDS/PMS activation results in the formation of ROS such as $SO_4^{\bullet-}$, $\bullet OH$, and $O_2^{\bullet-}$. This process leads to the 60 % removal of BTEX. A synergistic effect is reported when the BTEX/asphaltenes/PDS system is sonicated. This hybrid system results in the 97 % removal of BTEX in 360 min. The major mechanism in this process is the initial adsorption of BTEX on the asphaltenes surface. The adsorbed BTEX could then migrate to the cavitating bubble region (more details about the cavitating bubble and sonolysis are given in Section 2.5). The pyrolysis of oxidants during bubble collapse forms the reactive radical species and is able to degrade the BTEX by oxidation. In addition, the PDS as well as PMS could be activated by the asphaltenes by the electron transfer mechanism near the cavitating bubble.

Summarizing this part, the PS-based AOPs are simple to operate like the Fenton process. PDS is the major oxidant used in PS-AOPs. Sole PS-based processes can oxidize the AHs and therefore it can be implemented in the in situ chemical oxidation processes. The various activators such as Fe-, and other Fe-based, carbon-based materials, asphaltenes, UV, cavitation, etc. can activate the PS to generate the reactive species for the efficient degradation of AHs. The Fe^{2+}/PS system is the most effective process for the removal of AHs from both aqueous and soil matrices. Cavitation and microwave system were also effective, but, their large-scale implementation will be a difficult task.

3. AOPs for degradation of derivatives of PAHs

Derivatives of PAHs usually detected in environmental matrices are hydroxylated, chlorinated, nitrated, and methylated compounds. One of the important sources of derivatives of PAHs is the incomplete combustion of carbon-containing compounds and also by chemical and microbial transformation of parent PAHs. These are more persistent and toxic than the parent PAHs (Bekbolet et al., 2009). However, there is no ample amount of published work available for the degradation of PAHs derivatives.

Among the various derivatives of PAHs, the degradation of naphthol (a hydroxylated derivative of naphthalene) by AOPs has been studied well. Naphthalene undergoes microbial degradation to form hydroxyl derivatives (naphthol) and release them into the environment. In another way, these derivatives are directly used in the industry for the synthesis of dyes and insecticides (Croera et al., 2008). Thus, there are a lot of chances to find this derivative in the environmental matrices. The toxicological studies confirmed the toxicity of this compound to the living organism (Kang et al., 2016). In another perspective, the derivatives of PAHs especially the methyl, hydroxyl, nitro, and chloro reduce their chances of electrophilic reaction with the ROS and become more stable towards oxidative degradation. In addition, it is reported that the oxygenated derivatives of these compounds are more toxic. It is noted, that the oxygenated products are the initial products formed during the oxidative degradation of AHs

(Falciglia et al., 2016). Therefore, there is a risk of accumulation of these compounds in the aquatic matrix, if the oxidation process is not strong enough to degrade also these by-products. Thus, strong treatment techniques need to be addressed for such derivatives.

The g-C_3N_4 was used in the removal of 2-naphthol, an oxygenated derivative of naphthalene (Lan et al., 2019). 87 % of the derivative was removed after 1 h of visible light irradiation and a similar efficiency is reported even at five consecutive cycles. As in the previous cases of g-C_3N_4-based materials, the removal efficiency was strongly influenced by the calcination temperature. The key species formed during the photocatalytic process on the g-C_3N_4 are $\bullet OH$ and $O_2^{\bullet-}$. A composite of g-C_3N_4 with bismuth molybdate (Bi_2MoO_6) was active in the visible region, which is utilized for the removal of β-naphthol. This composite has a carbon sheet structure, useful to shuttle the electrons between the two semiconductor materials. In this case, >65 % degradation was reported (Ma et al., 2017). Another Z scheme heterojunction catalyst of $Bi@β$-Bi_2O_3/g-C_3N_4 has shown excellent visible light activity and was used for the degradation of 2,3-dihydroxy naphthalene. In this catalyst, the role of Bi was to shuttle the electron between β-Bi_2O_3 and g-C_3N_4. This study formation of $\bullet OH$ and $O_2^{\bullet-}$ as the major radical species responsible for 87 % degradation of the target pollutant in 100 min (Lan et al., 2020).

Degradation of anthraquinone using faceted TiO_2 was reported by Ye et al. and achieved 88 % removal. The efficiency was compared with (101) and (010) Faceted TiO_2 and more removal was reported at (010) Faceted TiO_2 (Ye et al., 2019). The PMS activation by nano-MoO_2 by an electron transfer process was useful in the removal of various NAP derivatives such as 1-methylnaphthalene (87 %), 1-nitronaphthalene (86 %), 1-chloronaphthalene (97 %), 1-naphthylamine (99 %), and 1-naphthol (77 %). The contributing ROS were $SO_4^{\bullet-}$, $\bullet OH$, $O_2^{\bullet-}$, and $^1O_2$ (Chen et al., 2021). Bekbolet et al. reported the photocatalytic degradation of nitro-derivatives of naphthalene using TiO_2 (Bekbolet et al., 2009). Different isomers of dinitronaphthalenes (diNN) such as 1,3-dinitronaphthalene, 1,5-dinitronaphthalene, and 1,8-dinitronaphthalene were studied. In this case 45 %, 60 % and 40 % removal were achieved for 1,3-diNN, 1,5-diNN, and 1,8-diNN respectively after 3 h of treatment.

Ce(III)/PMS system has been tested for the removal of NAP and the substituted NAP (1-methylnaphthalene (1-MN), 1-nitronaphthalene (1−NN), 1-naphthol (1-NAP), and 1-naphthylamine (1-NA)). Ce(III)/Ce(IV) redox cycle activated the PMS. Fast degradation of the AHs was reported and the degradation was found in the order NAP (92 %) < 1-MN (93 %) < 1-NN (97 %) < 1-NAP = 1-NA (100 %). The electron transfer of Ce(III) to PMS resulted in formation of the reactive species, especially $SO_4^{\bullet-}$, followed by $\bullet OH$. The singlet oxygen by the self-decomposition of PMS was also involved in the degradation of NAP and its derivatives (Chen et al. 2022). The Ce(IV) can be reduced to regenerate Ce(III) and abundant reactive species were formed (Eqs. (32)–(33)).

$$Ce(III) + HSO_5^- \rightarrow Ce(IV) + SO_4^{\bullet-} + OH^- \tag{32}$$

$$Ce(IV) + HSO_5^- \rightarrow Ce(III) + SO_4^{\bullet-} + OH^- \tag{33}$$
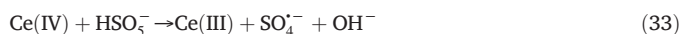
In summary, it is concluded that the AOPs are also effective for the degradation of PAHs derivatives. The major derivatives studied so far are the oxygenated and nitro-derivatives. Photocatalysis is the main AOPs studied for these derivatives. However, there is a research gap to study other AOPs and hybrid processes for these derivatives.

4. Comparison of degradation efficiencies of PAHs

The AOPs were found effective in the removal of AHs. However, the removal efficiency is varied with the structure, the substituents, and their position. In general, in the case of substituted AHs, depending on the electronic properties of the substituent, an electron-donating group (EDG) or electron-withdrawing group (EWG) substitute can be found (Manassir and Pakiari, 2019; Szatylowicz et al., 2019). A classical Hammett constant

is used to express the substitution effect (Krygowski et al., 2004). It can be expressed as (Eq. (34))

$$log \, \frac{k_x}{k_0} = \rho \times \sigma \qquad (34)$$

where k_x represents the apparent rate constant for the derivative and k_0 represents that of unsubstituted AHs. ρ and σ are the sensitivity constant and substitution constant respectively, which depends on the type and condition of the reaction and electron orientation. An electron-withdrawing ability increases with the increase of σ value and vice versa (Ren et al., 2022). Gągol et al. compared the removal of various AHs (BTEX, NAP, derivatives of AHs) using different AOP techniques (Gągol et al., 2018b). A visible difference in the degradation of these pollutants was observed in the pure cavitation processes. The degradation of AHs pollutants in cavitation-based AOPs followed the order of BTEX> Naphthalene $\gg$ -OH derivatives $\gg$ >-NO$_2$ derivatives.

As given in the previous sections, being a strong electrophile, the reactive species prefer to attack the electron-rich center in the compound. Any of the electron-donating functional groups (-OH, -NH$_2$, -CH$_3$) attached to the aromatic ring increases the electron density, which can increase the electron density and facilitate the electrophilic substitution reactions. On the other hand, the electron-withdrawing functionalities (-NO$_2$, -SO$_3$H, -COOH, etc.) decrease the electron density in the ring and therefore hard to undergo the electrophilic substitution reaction in the medium. Also, when the reactivities are of PAHs compared with mono AHs, there are many electrons-rich sites and the resonance structure makes it more feasible for the electrophilic substitution.

However, the degradation efficiencies further depend on the solubility and other physicochemical properties of the target compound and also the process applied for the degradation. As an example, as per the above statement, the phenols and phenol derivatives are hardly degraded in cavitation processes compared to benzene. But the opposite effect is likely due to the high volatility of the compound, which resists the degradation in the bubble interior. Similar results were reported for naphthalene likely due to their less aromaticity. Sponza et al. compared the sonochemical degradation of more hydrophobic PAHs (DahA and BghiP) and less hydrophobic PAHs (PHE, PY, CHR, ANT, and BbF) (Sponza and Oztekin, 2010). In this case, it was found that the removal efficiencies were decreased with an increase in the number of benzene rings in the structure. Briefly, the most hydrophobic PAHs have shown the lowest degradation rate. This is correlated with the water solubility of the PAHs. However, an increase in temperature led to an improvement in the removal efficiency for the hydrophobic PAHs. The functional group present in the AHs also had a significant influence on the radical-mediated electrophilic reactions. Thus, it is obvious that the degradation varies with the functional groups attached to the AHs.

5. Degradation of AHs in the presence of co-existing matrix components

The degradation of PAHs was also studied in the presence of co-existing compounds, normally occurring in the aqueous matrices, such as inorganic ions and organic species to propose the capability of AOPs in real wastewater treatment applications. The inorganic ions of major concern in this kind of AOPs are chloride (salinity), nitrate ions, nitrite ions, sulfate ions, bicarbonate, and carbonate ions. Among the cationic species, Fe and Ca^{2+} are dominant in this kind of real water. As the soil or water medium is considered, many organic matrices can interfere with PAHs removal. Generally, these compounds can either interact with the pollutants or compete for the reactive species and affect the removal efficiency in AOPs. The inorganic ions can scavenge the ROS to form a variety of secondary radicals as given in Fig. 8.

Therefore, the removal efficiency in the presence of these ions depends on the reactivity of the secondary ions towards the organic pollutants. Many of them scavenge the radicals, while chlorides are often revealed to participate in the degradation process. All the above hypotheses are depending on the type of AOPs applied. The matrix effect of AOPs like UV/H$_2$O$_2$ photolysis, Fenton, and photocatalysis are seemed to be similar and are given in Table 2.

The scavenging effect generally relates to decreased availability of •OH or SO$_4^{\bullet-}$, consumed by the anions in the aqueous phase, followed by the formation of a variety of secondary – less reactive - radicals (Eqs. (35)–(46)). These secondary radical species are selective and thus not so reactive as the primary ROS. Therefore, the degradation efficiency is decreased in most cases by the scavenging effect. Shemer et al. found the reduced degradation of PAHs in UV/H$_2$O$_2$ photolysis in the presence of HCO$_3^-$, Cl$^-$, SO$_4^{2-}$, and H$_2$PO$_4^-$/HPO$_4^{2-}$ by the scavenging effect (Shemer and Linden, 2007b). Fard et al. investigated the removal of BTEX in the presence of common groundwater cations and anions (SO$_4^{2-}$, Cl$^-$, NO$_3^-$, CO$_3^{2-}$, Na$^+$, K$^+$, Mg^{2+}, and Ca^{2+}) using photocatalysis (Alizadeh Fard et al., 2013a). All the co-existing matrices decreased the removal efficiency, and a more prominent effect was reported for SO$_4^{2-}$, CO$_3^{2-}$, Ca^{2+}, and Mg^{2+} ions. Nearly 100 % BTEX was removed after 45 min of the treatment by UV/TiO$_2$/H$_2$O$_2$ system in distilled water, but the efficiency was decreased to 55 % and 50 % respectively with the addition of CO$_3^{2-}$ and SO$_4^{2-}$. Similarly, divalent ions Ca^{2+} and Mg^{2+} decreased the removal efficiency to 70 %. The inhibitory effect of these ions is either due to the blocking of the active site or the competition effect by the ions. This is further reflected in the real contaminated water where the removal efficiency is less than the pure water. Several environmental factors such as carbonate ions, chloride ions, etc., have been investigated for the degradation of naphthalene in photocatalysis. The degradation of benzene by Fe(III)-SPC and Fe(II)-SPC was also negatively affected by the inorganic constituents especially the Cl$^-$ and HCO$_3^-$ present in the groundwater matrix (Fu et al., 2015; Fu et al., 2017). However, in the case of SPC activated with Fe^{2+}, and Fe(III) chelated with EDDS didn't show any significant difference in the removal efficiency of ethylbenzene in the presence of SO$_4^{2-}$, Cl$^-$, NO$_3^-$. But the bicarbonate ions marginally decreased the removal efficiency of benzene.

Similar results were also reported by Federov et al. during the degradation of BTEX by PMS activated by the hydrodynamic cavitation process (Fedorov et al., 2021). They found the retarding effect of inorganic ions on the degradation of BTEX by PS and PMS activated by the hydrodynamic cavitation process. According to their study, >90 % of the BTEX was
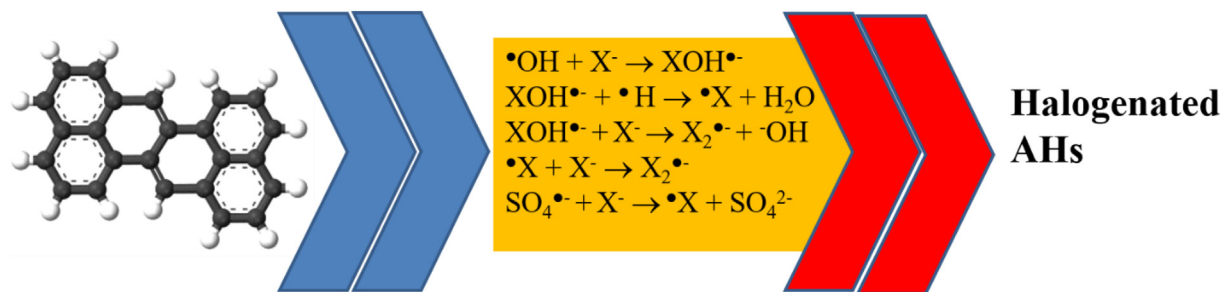

Fig. 8. Impact of halide ions on the degradation of PAHs during the AOPs.

Table 2

Impact of inorganic ions on the degradation of AHs by AOPs. The important observation and the role of the matrix are presented.
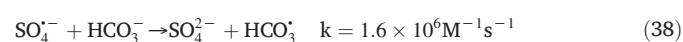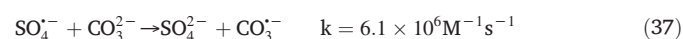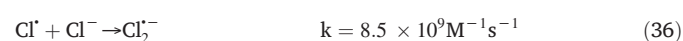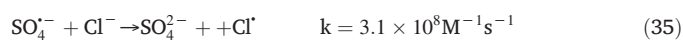
AOPs	AHs	Matrix	Important result	Role of matrix	Ref.
UV/H_2O_2					
	PAHs	Organic matter	Reduced the degradation of PAHs	Organic matters act as a UV filter that reduces the availability of UV light for H_2O_2 activation.	(Shemer and Linden, 2007b)
		CO_3^{2-}		CO_3^{2-} increases the alkalinity Strong scavenging of •OH	
Photocatalysis					
	BTEX	SO_4^{2-}, Cl^-, NO_3^-, CO_3^{2-}, Na^+, K^+, Mg^{2+} and Ca^{2+}	Decreased the removal efficiency	Blocking of the active site or competition effect by the ions	(Alizadeh Fard et al., 2013a)
	NAP	CO_3^{2-}, Cl^-	Carbonate ions decreased the removal efficiency and Cl^- increased the removal efficiency	Scavenging in the presence of CO_3^{2-} and salting-out effect in the presence of Cl^-	(Lair et al., 2008)
	ANQ	CO_3^{2-}, NO_3^-	CO_3^{2-} increased the removal	Carbonate radicals increased the removal	(Ye et al., 2019)
	ANQ	Fe^{3+}	Increased the removal	Increase in the photocatalytic activity due to the adsorption on the catalytic surface	(Ye et al., 2019)
Fenton and Fenton like system					
Fe^{2+}/H_2O_2	PHE, ANT, FLU	Cl-	Increased the removal efficiency	Reactive chlorine species are formed	(Lai et al., 2020)
Fe(III)-SPC and Fe(II)-SPC	B	Cl- and HCO_3^-	Decreased the removal efficiency	Scavenging effect	(Fu et al., 2015; Fu et al., 2017)
SPC activated with Fe^{2+}, and Fe(III) chelated with EDDS	E	CO_3^{2-}	Decreased the removal	Scavenging effect	(Cui et al., 2017a)
Fe(III)-SPC	Benzene	Humic acid	Increased the removal efficiency	Fe(III)-HA complex is formed. The Fe(II)/Fe(III) redox cycle reaction to increase the Fe^{2+} concentration	(Fu et al., 2015; Fu et al., 2017)
PS based AOPs					
Heat-activated PS	BTEX	Cl^- and Br^-	Increased the removal efficiency	Reactive Cl and Br species	(Ma et al., 2018)
Fe^{2+}/PMS	PHE, ANT, FLU	Cl^-	Increased the removal with the formation of toxic chlorinated products	Reactive chlorine species are formed	(Lai et al., 2020)
Ce(III)/PMS	NAP and its derivatives	Cl^-, NO_3^-, $HCO3^-$ and humic acid	The effect depends on the functional group	Secondary radicals are formed	(Chen et al., 2022)
Cavitation-PS	BTEX	Cl-, HCO_3^-, NO_3^- SO_4^{2-}, and $H_2PO_4^-$/HPO_4^{2-}	Decreased the removal	Scavenging effect	(Fedorov et al., 2021)

degraded with HC-PS and HC-PMS processes. However, the addition of Cl^- ions decreased the removal efficiency of benzene, toluene, ethylbenzene, and xylene to 17, 43, 46, and 58 % respectively. However, NO_3^- SO_4^{2-}, and $H_2PO_4^-$/HPO_4^{2-} didn't have any effect on the removal in the processes. Like in the previous cases, CO_3^{2-} and HCO_3^- and NOM reduced the removal efficiency. Moreover, the degradation of AHs in the presence of inorganic ions resulted in the formation of many toxic halogenated derivatives.

On the other hand, the secondary radicals sometimes show higher reactivity towards the AHs based on their functionalities. An enhanced degradation is observed in such cases. The removal efficiency of anthraquinone was increased with the addition of bicarbonate ions in TiO_2-aided photocatalysis (Ye et al., 2019). The bicarbonate ions scavenge the •OH to form a carbonate radical, which is also capable of reacting with the organics (Buxton et al., 1988). The advantage is that this radical possesses a longer lifetime compared to hydroxyl radical and thus, can react with the pollutants in the solution phase (Chen et al., 1975; Haygarth et al., 2010).

Ma et al. detailed the effect of inorganic anions on the removal of BTEX by heat-activated PS (Ma et al., 2018). The inorganic ions such as Cl^- and Br^- had a positive effect on the removal efficiency except for benzene. A significant increase was observed for xylene, an increase of rate from 0.01 min^{-1} to 0.2 min^{-1} with the addition of 500 mM of Br^-. But for benzene, these ions decreased the removal efficiency. The Br^- generally decreases the initial pH of the solution to the most suited for $SO_4^{•-}$ radical reaction. In addition, the bimolecular rate constant for the reaction of $SO_4^{•-}$ with Br^- (3.5×10^9 M^{-1} s^{-1}) is ten times higher than that with Cl^- ions (3.1×10^8 M^{-1} s^{-1}) (Ma et al.,

2018). Among the BTEX, benzene is a less electron-rich compound, and thus decrease in the SO_4^{2-} concentration decrease the degradation of benzene. On the other hand rest of the compounds are highly electrophilic and the oxidation occurs rapidly by the secondary radicals of Cl and Br. Lai et al. reported the degradation of PAHs (such as phenanthrene, anthracene, and fluoranthene) using the Fenton process in the presence of varying Cl^- concentrations (Lai et al., 2020). In their previous study, they optimized the Fe^{2+}/H_2O_2 ratio and Fe^{2+}/PMS ratio as 1 for the removal of the above three PAHs with an H_2O_2 concentration of 30 mM and PMS concentration of 1 mM. The total PAHs removals were 78 % and 65 % respectively for the Fe^{2+}/H_2O_2 ratio and Fe^{2+}/PMS processes. Total PAHs removal was significantly increased with Cl^- ion content in the medium in the Fe^{2+}/PMS system with the generation of free chlorine in the system. Reactive chlorine species and reactive oxygen species are in the reaction processes. Moreover, $Fe^{2+}/H_2O_2/$ Cl^- is not generating any chlorinated products, thus toxicity is not increased like other chlorination reactions. On the other hand $Fe^{2+}/PMS/Cl^-$ generates many chlorinated products and toxicity is increased.

$$SO_4^{•-} + Cl^- \rightarrow SO_4^{2-} + +Cl^• \qquad k = 3.1 \times 10^8 M^{-1}s^{-1} \qquad (35)$$

$$Cl^• + Cl^- \rightarrow Cl_2^{•-} \qquad k = 8.5 \times 10^9 M^{-1}s^{-1} \qquad (36)$$

$$SO_4^{•-} + CO_3^{2-} \rightarrow SO_4^{2-} + CO_3^{•-} \qquad k = 6.1 \times 10^6 M^{-1}s^{-1} \qquad (37)$$

$$SO_4^{•-} + HCO_3^- \rightarrow SO_4^{2-} + HCO_3^• \qquad k = 1.6 \times 10^6 M^{-1}s^{-1} \qquad (38)$$

$$HCO_3^{\bullet} \leftrightarrow H^+ + CO_3^{\bullet-} \tag{39}$$

$$SO_4^{\bullet-} + Br^- \rightarrow SO_4^{2-} + Br^{\bullet} \qquad k = 3.5 \times 10^9 M^{-1}s^{-1} \tag{40}$$

$$OH^- + Br^{\bullet} \rightarrow HBrO^{\bullet-} \qquad k = 1.1 \times 10^{10} M^{-1}s^{-1} \tag{41}$$

$$Br^{\bullet} + Br^- \rightarrow Br_2^{\bullet-} \qquad k = 1.1 \times 10^{10} M^{-1}s^{-1} \tag{42}$$

$$Br_2^{\bullet-} + Br^{\bullet} \rightarrow Br_2 + Br^- \qquad k = 2 \times 10^9 M^{-1}s^{-1} \tag{43}$$

$$2Br_2^{\bullet-} \rightarrow Br_2 + 2Br^- \qquad k = 1.9 \times 10^9 M^{-1}s^{-1} \tag{44}$$

$$2Br^{\bullet} \rightarrow Br_2 \qquad k = 1.0 \times 10^9 M^{-1}s^{-1} \tag{45}$$

$$HO^{\bullet} + NO_3^- \rightarrow H_2O + NO_3^{\bullet-} \qquad k = 5 \times 10^5 M^{-1}s^{-1} \tag{46}$$
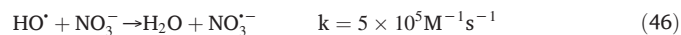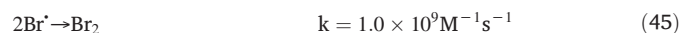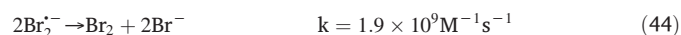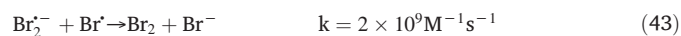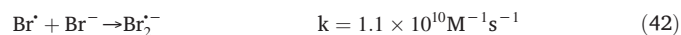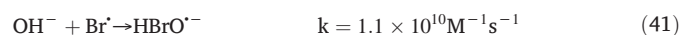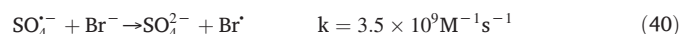
In addition, some inorganic ions affect the reaction site on the photocatalytic materials and influence the reactive species formation. It has been found that the presence of certain inorganic ions, like Cl^- ion, increases the accumulation of organics on the solid surface through the salting-out effect. Lair et al. found an enhanced photocatalytic degradation of naphthalene from 70 % to 99 % with an increasing Cl^- concentration from 0 M to 1.2 M. The role of the salting-out effect was confirmed by the adsorption study in the presence of these ions. It was found that the adsorption of NAP on the surface increased with an increase of Cl^-. Thus, it is obvious that the salting-out effect has a significant role in the photocatalytic degradation of pollutants. Similarly, the Fe^{3+} present in the water matrix had a positive effect in this kind of photocatalytic system. The Fe^{3+} was adsorbed on the TiO_2 surface and acted as an electron acceptor. The photogenerated electrons were then stored on the adsorbed Fe^{3+}, and it reacted with O_2 to form $O_2^{\bullet-}$. In addition, the H_2O_2 generated from the Fe^{3+}/Fe^{2+} redox process enhanced the degradation.

In cavitation-based processes, in addition to the scavenging effect of the inorganic ions, there could be many other possibilities. The interface region of the bubbles and the liquid region are the major places of degradation in the case of PAHs. Therefore, any parameter that influences the AH to be in either of the above regions affects the degradation (Rayaroth et al., 2018; Seymour and Gupta, 1997). The physicochemical properties of the interfering matrix that tends to drag the interface region of the cavitating bubble affect the degradation of PAHs in sonolysis. In addition, the salting-out effect of anions pushes the contaminants to the highly reactive region of the cavitating bubble and has a positive effect. Dissolved oxygen has a prominent effect on the degradation of PAHs. The initial step in the generation of ROS is the homolytic cleavage of the O_2 molecule to atomic oxygen, which reacts rapidly with water to form •OH. Thus, the dissolved oxygen increases the number of available reactive species in the medium.

A comparison of the EAOPs with and without the use of Cl^- was reported. The Cl^- ion was revealed to have a significant role in the processes. The electrolyte (NaCl) enhanced the removal efficiency to 93 % (only 74 % was observed without NaCl) due to the evolution of reactive chlorine species as given in Eqs. (47)–(50).

$$2Cl^- \rightarrow Cl_2 + 2e^- \tag{47}$$

Under acidic pH,

$$Cl_2 + H_2O \rightarrow HClO + H^+ + Cl^- \tag{48}$$

Under alkaline pH,

$$Cl_2 + 2OH^- \rightarrow ClO^- + Cl^- + H_2O \tag{49}$$

$$HClO + OH^- \rightarrow ClO^- + 2H^+ + 2e^- \tag{50}$$
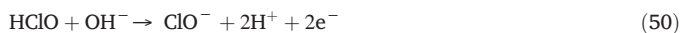
Like normal Fenton processes, acidic pH practically favors good removal efficiency due to the formation of strong oxidant HClO. Muff et al.

reported the electrochemical degradation of PAHs such as naphthalene, pyrene, and fluoranthene in saline water conditions using Ti/Pt90-Ir10 anode (Muff and Søgaard, 2010). The degradation efficiency was increased under acidic pH with the formation of chlorinated PAHs. Moreover, the degradation and formation of these chlorinated products depend on the solubility of the PAHs. Naphthalene undergoes nearly complete degradation in 240 min of electrolysis, whereas the other two PAHs didn't undergo complete degradation even after 240 min. The chlorinated naphthalene was formed in this case as well. In the same way, Tawabini et al. studied the removal of BTEX using EAOP with a BDD electrode (Tawabini et al., 2020). The degradation of BTEX after 15 min of electrolysis followed the order xylene > ethyl benzene > toluene > benzene with a current density of = 100 mA/cm². The high saline condition resulted in the in situ generations of various oxidants such as H_2O_2, and active chlorine species which fasten the degradation.

In contrast to the inorganic matrix, the organic matter (Humic acid, HA) enhanced the removal efficiency of benzene in this system. The HA may increase the availability of Fe in the solution with the formation of a Fe(III)-HA complex. The time required for the complete degradation of benzene in Fe(III)-SPC was 100 min in the control experiment, but degradation the time is decreased to 30 min in the presence of HA. The chelation of Fe by HA increases the availability of Fe in solution for SPC activation. In addition, the phenolic or quinone group present in the HA favors the Fe(II)/Fe(III) redox cycle reaction to increase the Fe^{2+} concentration in the medium for the reaction. On the other hand, the efficiencies of Fe^{2+}-SPC and Fe(III)-EDDS-SPC systems for the removal of benzene are decreased in the presence of NOM (Cui et al., 2017a). Shemer et al. found that the organic matters reduced the degradation of PAHs like other AOPs (Shemer and Linden, 2007b). Moreover, the organic matters act as a UV filter that reduces the availability for the H_2O_2 activation. Another factor when considering the real water matrix is the alkalinity of the solution.

The removal was also affected by the presence of HA, benzoic acid, pentane, and pentanol in cavitation-based AOPs. The binding of organic matrices with PAHs significantly affects the removal. This happens in the case of HA, which reduces the availability of PAHs from the interface region of the cavitating bubble. In addition, the •OH scavenging effect of HA and benzoic acid further reduces the removal efficiency. Ke et al. studied the removal of PAHs from sludge matrix containing soil organic matters using the sono-Fenton process (Ke et al., 2018). Nearly 84 % and 32 % of the PAHs were removed during this hybrid process. It shows the competition of soil organic matter (SOM) and PAHs for the reactive species. As discussed previously the interaction of PAHs with SOM played a significant role in their removal in such a complex matrix. In addition, the SOM with high tryptophan-like and tyrosine-like moieties regenerates Fe^{2+} in the system through the electron transfer mechanism. In summary, the co-existing ions present in the matrix affect the degradation based on the nature of the process and target compound. The inorganic ions scavenged the reactive species and decreased the removal efficiency in most of the AOPs. On the other hand, the reactive Cl, and Br radical species formed during the oxidation of Cl- and Br- containing matrices increased the removal of AHs. However, a formation of halogenated products has been reported. The humic acids had a role in the degradation in Fe-containing systems through the Fe(II)/Fe(III) redox cycle.

6. Degradation products and mechanism

In •OH-, and PS-based AOPs, the primary step is one-electron oxidation of the aromatic ring of PAHs to form corresponding radical cations. The major intermediate products of PAHs are phenolic, quinone, alcohols, aliphatic acids, etc. As explained in the selected AOPs for the degradation of PAHs, the major species involved are hydroxyl radicals, sulfate radicals, superoxide radicals, singlet oxygen, etc. Among them, hydroxyl radicals react non-selectively with the organics (H abstraction, hydroxylation, electron transfer, etc.) (Cooper et al., 2009; Fatta-Kassinos et al., 2011). The sulfate radical degrades the pollutant through the electron transfer reaction. On

the other hand, superoxide radicals, and singlet oxygen react to the pollutants via the H abstraction and electrophilic attack respectively. Chen et al. studied the degradation mechanism of a PAH, BaP by •OH and $^1O_2$ using this DFT (Chen et al., 2020). The preferable position for the OH radicals was predicted by the density functional theories (DFT). The Fukui function is calculated based on the DFT calculations. Electrophilic Fukui function (FK^- = ρ_{HOMO} (r)) is used to describe the interaction between reactants in AOPs. The Fukui function can be calculated from the population of atom k in the neutral $q_{k(N)}$ and cation $q_{k(N-1)}$ species from the Eq. (51) (Fig. 9).

$$f_k^- = q_{k(N)} - q_{k(N-1)} \tag{51}$$

As suggested by the DFT and Fukui function, the electron-rich center C6 is the preferred position for the attack of reactive species (Fig. 9). The hydrogen abstraction possibilities are neglected because of their high reaction energies. The •OH attacks at the C6 position to form C6-OH as the main intermediate product and $^1O_2$ led to the formation of a highly reactive zwitterion product, BaP-6-OO. It is reported that the rate constant for the formation of BaP-6-OO (1.70×10^{-5} cm³·molecule⁻¹·s⁻¹) is higher than that for the BaP-6-OH (1.65×10^{-10} cm³·molecule⁻¹·s⁻¹). These intermediates further undergo a reaction with the reactive species to form the phenolic or ketonic products (Chen et al., 2020).

In the case of sulfate radical, an initial reaction of sulfate radical with water molecule results in formation of a pre-complex (solvated sulfate radical) (Eq. (52)). This pre-complex is responsible for attack on the carbon atom with lower Gibbs free energy, and is transformed into post reactive complex with the transformation product (Eq. (53)) (Liu et al., 2019).
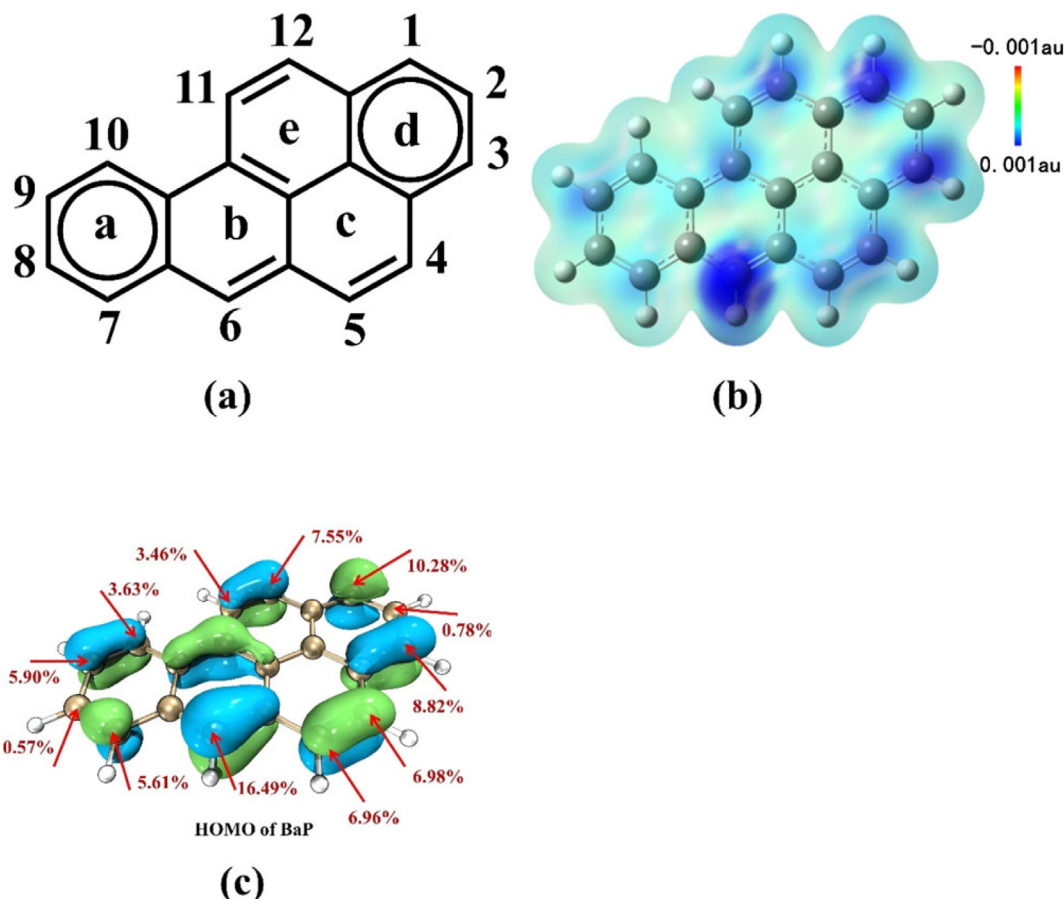
$$SO_4^{\cdot-} + H_2O \rightarrow SO_4^{\cdot-} \cdot H_2O \tag{52}$$

$$SO_4^{\cdot-} \cdot H_2O + PAH \rightarrow PAH \cdot SO_4^{\cdot-} \cdot H_2O \rightarrow \text{reaction product} \tag{53}$$
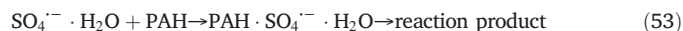
The oxidative degradation BaP yields hydroxylated products, hydroquinones, as the primary intermediate products. The continuous oxidation leads to the formation of ring open products and finally to short-chain acids. The mechanism could be illustrated in Fig. 10 by taking BaP as the model PAH. Methyl derivatives of PAHs also undergo a similar pathway and form similar products as that of the parent PAH (Chen et al., 2021). But chlorinated and nitrated PAHs initially form chlorinated or nitrated intermediate and undergo normal products as that of PAHs. As an example, oxidation of nitronaphthalene resulting the formation of several hydroxylated products and naphthyl amine. Thus, special consideration should be given to the PAHs derivates, which tend to form toxic intermediates.

7. Cost-effectiveness of AOPs in PAHs degradation

Economic feasibility is an important parameter in any water treatment process while installing the process in large-scale applications (Alalm et al., 2021). The concentration of the target contaminants and other by-products, and total organic content in the effluent should be minimized to an acceptable limit during the oxidation – dependent on local regulations. Therefore, the cost of the process highly depends on the time required to achieve the above limits. It depends on the initial concentration of the pollutants, nature, and source of the polluted water, and the daily discharge amount. In AOPs, the cost is mainly related to the chemicals used (For e.g.: PS, H_2O_2, Fe^{2+}, precursors for the synthesis of nanomaterials), equipment (photo and cavitation reactors), their maintenance, and the electricity or energy consumption costs. The capital cost in any of the processes covers the civil and mechanical works, buildings, engineering designs and supervision of on-site infrastructure, start-up costs (equipment), and working capital

Fig. 9. Numbering (a), electronic structure (b), and HOMO of BaP (c) were obtained by the DFT calculation. The blue portion indicates the electron centers and the intensity is decreased with a decrease of the energy value (Reprinted with the permission from (Chen et al., 2020)).
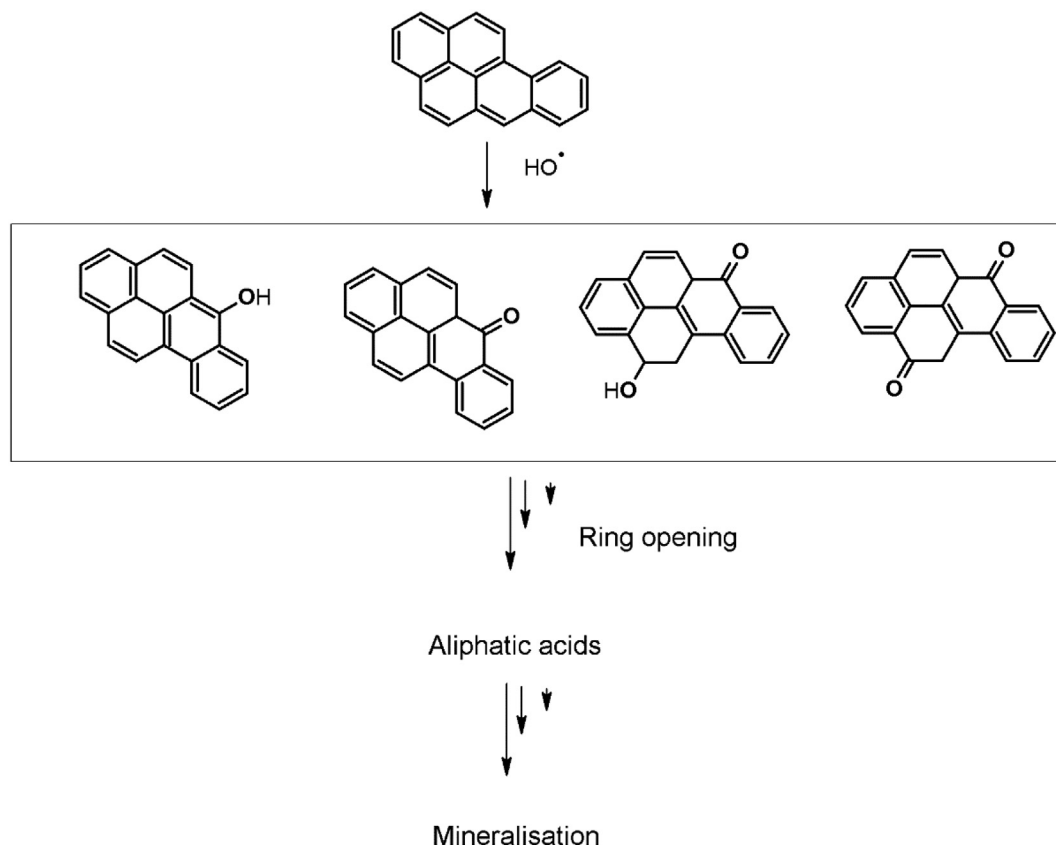
Fig. 10. The primary intermediate formed and their mechanism of formation during the degradation of BaP induced by •OH based on the DFT study.

(Krichevskaya et al., 2011). The cost of H_2O_2, PS, $FeSO_4$, .$7H_2O$, ZVI, citrate, H_2SO_4, and NaOH, 40.70 €/L, €77.10/1 kg, 91.2 €/kg, €5/g, 75.2 E/kg, 2 €/Kg, 0.55 €/Kg, and 2.05 €/Kg respectively. The cost of electricity for industrial customers in Poland in 2021 is 0.1092 euro cent per 1 kWh. The capacity of any of the reactor are estimated from the volumetric treated wastewater amount per year (V_t), the operation time (T_t), working time per day for the reactor (t_w), and number of working days per year (D) (Eq. (54)).

$$C = V_t \times \frac{T_t}{T_w \times D} \tag{54}$$

The energy cost (EC) is calculated from the required power to circulate the wastewater and the unit price of energy (Eq. (55)).

$$EC = EP_i \times T_w \frac{D}{V_t} \tag{55}$$

It is clear from the previous sections, that the time required for >90 % degradation of PAHs from an aqueous medium is 40 min–8 h. On the other hand, in the soil matrix, >24 h are required to achieve the same

efficiency. The optimized parameters for the best treatment method in the reviewed papers and the estimated costs are given in Table 3. Analysis of these data reveals, that the best methods were UV/H_2O_2, Fenton ZVI/H_2O_2, sonolysis, and Fe^{2+}-CA/PS from an aqueous medium. On the other hand, processes such as microwave-PS and ZVI-PS were found to be effective for the removal of the soil matrix. Energy consumption is included in the processes in power-based processes. It is clear that the most economically viable process was found to be Fe(II)-CA-PS (11.76 €/m³), followed by sonolysis (28.04 €/m³) and UV photolysis (36.4166 €/m³). The cost of $ZVI-H_2O_2$ is mainly raised from the synthesis cost of ZVI. The cost of soil treatment using microwave-activated PS is estimated to be ~80 €/kg and that of ZVI-PS is 390 €/kg. However, the estimation for soil treatment is appropriate for in situ treatment. It does not include an important aspect - out of the scope of this review - transport of treated soil in case of off-line applications.

In addition, we have compared the other processes with structurally similar compounds for the scaling up of the process. The treatment cost of ozone-based AOPs for phenols is reported as 2.1€/m³ that is further varied with the initial concertation of pollutants in the water source (Andreozzi et al., 1996). The cost for the treatment of 5 mg/L of phenol is 5.1€/m³,

Table 3
Cost for the treatment of AHs.

Processes	C_0	Time (min)	Treated volume (L)	% degradation	Amount of chemicals	Cost of chemical [€/m³]	Energy consumption [kWh/m³]	Cost of energy [€/m³]	Total cost of treatment [€/m³]
UV/H_2O_2	100 mgL^{-1}	180	4	90 %	$[H_2O_2]$ = 300 mg/L	35.8	5.5	0.6	36.4
$nZVI-H_2O_2$	4 mgL^{-1} pH 3	20	1	99 %	nZVI 150 mg/ L, and H_2O_2 9.0 mM	786.6	Negligible	Negligible	786.6
sonolysis	30 mg/L	120	1	95 %	–	–	256.7	28.0	28.0
Fe(II)-CA-PS	0.10 mM.	120	0.25	100 %	$[Fe(II)]_0$ = 0.50 mM, $[CA]_0$ = 0.10 mM, $[PS]_0$ = 1.50 mM,	11.7	Negligible	Negligible	11.7

but when the concentration is increased to 100 mg/L the cost is increased to 100 €/m^3 (Krichevskaya et al., 2011). Bustillo-Lecompte et al. have estimated the electrical energy consumption for the degradation of BTEX using UV-254 and UV-185/H$_2$O$_2$ at various oxidant concentrations (Bustillo-Lecompte et al., 2018). Among the selected UV sources, UV-185 had a lower electrical energy consumption of 3.5 kWh/m^3 and thus lower operational costs. On the other hand, land requirements for the installation and/or the number of UV lamps (with 4 kW and 20,000-h of a lifetime each) should be considered in photochemical oxidation degradation/treatment processes (Silva et al., 2016). The estimated cost for the treatment of phenol real wastewater by a solar photo Fenton process is 6€/m^3 (Silva et al., 2016). For the hybrid photocatalytic process, the estimated cost was reported to be 39.89€/m^3. On the other hand, the cost of cavitation-based AOPs is 0.017€/m^3 which is limited to bath and horn-type reactor with a capacity of 0.1 to 2.5 L. The energy consumption and the costs are high for the highly concentrated wastewater and the bicarbonate-rich and other complex water and seawater. When the sono reactor is replaced with a hydrodynamic reactor the cost can be reduced to 0.01 to 0.02 €/m^3 with the use of a venturi tube (Gągol et al., 2018b). The PS-based AOPs are applied in the soil as in situ chemical oxidants. The cost in this process includes site preparation, mobilization/demobilization (transportation to site, mobile office, storage, fabrication, assembly, setup, dismantle, well abandonment), equipment and labor cost, chemicals, equipment maintenance, power, etc. The estimated overall cost for such kind of ISCO was reported to be 304€/kg (Gavaskar et al., 2008; Stephen Rosansky, 2010). In short, the Fenton-based AOPs are the cost-effective method for the treatment of PAHs. The cost was further reduced with the use of chelating agents as it reduced the oxidant dose. Even though ZVI-based methods are effective in the complete removal of the AHs, their cost of synthesis and other parameters are of important concern. The catalytic and sonocavitation processes are not cost-effective because of the large energy consumption.

8. Future suggestions and recommendations

As given in this review, the AOPs were found to be effective for the removal of AHs and their derivatives. The AOPs such as UV/H$_2$O$_2$ photolysis, photocatalysis, Fenton, and activated PS methods, were reported as the most effective processes. However, most of the works has been studied in the lab-scale and more efforts are needed in the scaling up of each process. Other aspects needed to be justified in the future paper are listed below.

1. Since the concentration of the pollutants varied concerning the source of contamination and nature of the water sources, the optimization of oxidants to pollutants molar ratio (Rox) is important in any of the processes.
2. The separation of the catalyst after the photocatalytic process is a challenge. Therefore, the reactors should be constructed, keeping in mind this feature. The coating/immobilization of the photocatalyst on the reaction vessel can solve a part of the problem. The metal ions leaching is another issue in using metal-doped photocatalysts, as it can cause toxicity with respect to the aquatic system. Therefore, continuous monitoring for the metal species leaching is a must.
3. PS and cavitation-based AOPs led to the complete degradation of AHs. On the other hand, it is known that cavitation conditions can cause the formation of intermediate products with higher toxicity. This should be addressed by the intermediate product analysis, toxicity studies, and TOC analysis. However, the synergistic applications of AOPs with other oxidants like O$_3$ should be effective in minimizing the formation of toxic intermediates
4. Several studies reported the formation of unexpected nitro-product formation in nitrite ions containing water sources (Rayaroth et al., 2022) and many halogenated products in the presence of excess halide ions (Lai et al., 2020). Therefore, a complete understanding of these parameters is necessary before the implementation of developed processes on the industrial scale.
5. The hybrid processes are most effective for AHs to achieve complete mineralization as well as to reduce the time of operation.

9. Conclusion

There are multiple sources of AHs causing the accumulation of PAHs in soil and water. The advanced oxidation processes were successfully employed for the removal of PAHs from both water and soil matrices. This paper reviewed all the available information on the degradation studies of PAHs using AOPs such as UV/H$_2$O$_2$ photolysis, photocatalysis, Fenton, PS-based processes, etc. This review also considered the various derivatives of AHs. In comparison with other removal methods like physical and biological methods, the degradation rate in AOPs is high and complete degradation occurred within a short period. The processes can be performed in environmentally relevant conditions as well. Even though there are many photocatalytic materials tested for the degradation of AHs on laboratory scale, their scale-up is still under investigation. The sonochemical methods were stepped back in the removal of AHs due to their high operational cost. Therefore, among the reviewed papers, it is concluded that PS-based AOPs and EAOPs were effective in the removal of contaminants from an aqueous medium. The strong interaction between the AHs and soil makes it hard to remove from the soil matrix. Therefore, several methods adopted the use of suitable solubilizing agent-assisted oxidation methods. In such cases, the PS is the first and best option.

The removal efficiencies of the AHs in AOPs further depend on their structure. The initial reaction of •OH with AHs leads to the phenolic compounds and is followed by the ring-opening reaction. In addition, a variety of reactive species take part in the degradation of AHs in AOPs. The involvement of superoxide radicals and singlet oxygen in AOPs like SR-AOPs and photocatalysis were favored for rapid oxidation especially the aniline derivates of AHs. The quinone derivates formed during the oxidation of AHs are an important activator of PS, which enhanced the generation of reactive species in the medium. The monoaromatic compounds undergo rapid oxidation compared to low and high molecular weight PAHs and their derivatives. In addition, the removal efficiency was affected by the various matrices such as organic and inorganic ions. The major constituents of the water matrices such as bicarbonate ions and the organic species scavenged the reactive species and reduced the removal efficiencies in most of the cases. However, for some of the hydroxylated and amino derivatives of AHs, the carbonate radicals improved the removal efficiency via the electron transfer mechanism. The halide ions and nitrite ions affected the removal badly as well as causing the formation of toxic halogenated and nitro derivatives. In addition, the de-nitration/halogenation processes in many of the respective AHs derivatives generate many toxic intermediates. Therefore, much more attention should be given to the removal of derivatives of AHs.

CRediT authorship contribution statement

Manoj P. Rayaroth: Conceptualization, Methodology, Visualization, Writing – original draft. **Mateusz Marchel:** Writing – review & editing. **Grzegorz Boczkaj:** Conceptualization, Methodology, Project administration, Supervision, Writing – review & editing.

Data availability

No data was used for the research described in the article.

Declaration of competing interest

The authors declare that they have no known competing financial interests or personal relationships that could have appeared to influence the work reported in this paper.

Acknowledgments

Appendix A. Supplementary data

Supplementary data to this article can be found online at https://doi.org/10.1016/j.scitotenv.2022.159043.

References

Abbas, W., Abbas, S., Nawaz, M., Azam, M., Oh, J.-M., Shahzad, A., 2021. Development of polystyrene coated persulfate slow-release beads for the oxidation of targeted PAHs: effects of sulfate and chloride ions. J. Hazard. Mater. 416, 125879.

Abdel-Shafy, H.I., Mansour, M.S.M., 2016. A review on polycyclic aromatic hydrocarbons: source, environmental impact, effect on human health and remediation. Egypt. J. Pet. 25, 107–123.

Adeola, A.O., Forbes, P.B.C., 2021. Advances in water treatment technologies for removal of polycyclic aromatic hydrocarbons: existing concepts, emerging trends, and future prospects. Water Environ. Res. 93, 343–359.

Agarwal, P., Anand, M., Chakraborty, P., Singh, L., Masih, J., Taneja, A., 2022. Placental levels of polycyclic aromatic hydrocarbons (PAHs) and their association with birth weight of infants. Drug Chem. Toxicol. 45, 868–877.

Ajab, H., Isa, M.H., Yaqub, A., 2020. Electrochemical oxidation using Ti/RuO2 anode for COD and PAHs removal from aqueous solution. Sustain. Mater. Technol. 26, e00225.

Alalm, M.G., Djellabi, R., Meroni, D., Pirola, C., Bianchi, C.L., Boffito, D.C., 2021. Toward scaling-up photocatalytic process for multiphase environmental applications. Catalysts 11, 562.

Alizadeh Fard, M., Aminzadeh, B., Vahidi, H., 2013a. Degradation of petroleum aromatic hydrocarbons using TiO2 nanopowder film. Environ. Technol. 34, 1183–1190.

Alizadeh Fard, M., Torabian, A., Bidhendi Gholam Reza, N., Aminzadeh, B., 2013b. Fenton and photo-Fenton oxidation of petroleum aromatic hydrocarbons using nanoscale zero-valent iron. J. Environ. Eng. 139, 966–974.

Alves, C.A., Vicente, A., Custódio, D., Cerqueira, M., Nunes, T., Pio, C., et al., 2017. Polycyclic aromatic hydrocarbons and their derivatives (nitro-PAHs, oxygenated PAHs, and azaarenes) in PM2.5 from Southern European cities. Sci. Total Environ. 595, 494–504.

Andreozzi, R., Caprio, V., Insola, A., 1996. Kinetics and mechanisms of polyethyleneglycol fragmentation by ozone in aqueous solution. Water Res. 30, 2955–2960.

Arumugam, M., Natarajan, T.S., Saelee, T., Praserthdam, S., Ashokkumar, M., Praserthdam, P., 2021. Recent developments on bismuth oxyhalides (BiOX; X = Cl, Br, I) based ternary nanocomposite photocatalysts for environmental applications. Chemosphere 282, 131054.

Bahmani, M., Bitarafhaghighi, V., Badr, K., Keshavarz, P., Mowla, D., 2014. The photocatalytic degradation and kinetic analysis of BTEX components in polluted wastewater by UV/H2O2-based advanced oxidation. Desalin. Water Treat. 52, 3054–3062.

Bai, H., Zhou, J., Zhang, H., Tang, G., 2017. Enhanced adsorbability and photocatalytic activity of TiO2-graphene composite for polycyclic aromatic hydrocarbons removal in aqueous phase. Colloids Surf. B: Biointerfaces 150, 68–77.

Bai, X., Sun, H., Sun, J., Zhu, Z., 2022. Efficient removal of sixteen priority polycyclic aromatic hydrocarbons from textile dyeing sludge using electrochemical Fe2 + -activated peroxymonosulfate oxidation-a green pretreatment strategy for textile dyeing sludge toxicity reduction. J. Hazard. Mater. 435, 129087.

Bajagain, R., Jeong, S.-W., 2021. Degradation of petroleum hydrocarbons in soil via advanced oxidation process using peroxymonosulfate activated by nanoscale zero-valent iron. Chemosphere 270, 128627.

Banerjee, S., Pillai, S.C., Falaras, P., O'Shea, K.E., Byrne, J.A., Dionysiou, D.D., 2014. New insights into the mechanism of visible light photocatalysis. J. Phys. Chem. Lett. 5, 2543–2554.

Bekbolet, M., Çınar, Z., Kılıç, M., Uyguner, C.S., Minero, C., Pelizzetti, E., 2009. Photocatalytic oxidation of dinitronaphthalenes: theory and experiment. Chemosphere 75, 1008–1014.

Boczkaj, G., Fernandes, A., 2017. Wastewater treatment by means of advanced oxidation processes at basic pH conditions: a review. Chem. Eng. J. 320, 608–633.

Brillas, E., Sirés, I., Oturan, M.A., 2009. Electro-Fenton process and related electrochemical technologies based on Fenton's reaction chemistry. Chem. Rev. 109, 6570–6631.

Burdin, F., Tsochatzidis, N.A., Guiraud, P., Wilhelm, A.M., Delmas, H., 1999. Characterisation of the acoustic cavitation cloud by two laser techniques. Ultrason. Sonochem. 6, 43–51.

Bustillo-Lecompte, C.F., Kakar, D., Mehrvar, M., 2018. Photochemical treatment of benzene, toluene, ethylbenzene, and xylenes (BTEX) in aqueous solutions using advanced oxidation processes: towards a cleaner production in the petroleum refining and petrochemical industries. J. Clean. Prod. 186, 609–617.

Buxton, G.V., Greenstock, C.L., Helman, W.P., Ross, A.B., 1988. Critical review of rate constants for reactions of hydrated electrons, hydrogen atoms and hydroxyl radicals (·OH/·O− in aqueous solution. J. Phys. Chem. Ref. Data 17, 513–886.

Byrne, C., Subramanian, G., Pillai, S.C., 2018. Recent advances in photocatalysis for environmental applications. J.Environ.Chem.Eng. 6, 3531–3555.

Cai, H., Sun, L., Wang, Y., Song, T., Bao, M., Yang, X., 2019. Unprecedented efficient degradation of phenanthrene in water by intimately coupling novel ternary composite Mn3O4/MnO2-Ag3PO4 and functional bacteria under visible light irradiation. Chem. Eng. J. 369, 1078–1092.

Chakraborty, P., Sampath, S., Mukhopadhyay, M., Selvaraj, S., Bharat, G.K., Nizzetto, L., 2019. Baseline investigation on plasticizers, bisphenol A, polycyclic aromatic hydrocarbons and heavy metals in the surface soil of the informal electronic waste recycling workshops and nearby open dumpsites in Indian metropolitan cities. Environ. Pollut. 248, 1036–1045.

Chen, S.-N., Hoffman, M.Z., Parsons, G.H., 1975. Reactivity of the carbonate radical toward aromatic compounds in aqueous solution. J. Phys. Chem. 79, 1911–1912.

Chen, X.-M., Chu, Y.-J., Liu, C.-G., 2020. Degradation mechanism of benzo[a]pyrene initiated by the OH radical and 1O2: an insight from density functional theory calculations. ACS Omega 5, 25552–25560.

Chen, X., Vione, D., Borch, T., Wang, J., Gao, Y., 2021. Nano-MoO2 activates peroxymonosulfate for the degradation of PAH derivatives. Water Res. 192, 116834.

Chen, X., Wang, P., Peng, F., Zhou, Z., Waigi, M.G., Ling, W., 2022. Ce(III) activates peroxymonosulfate for the degradation of substituted PAHs. Chemosphere 306, 135525.

Cheng, H., Deng, Z., Chakraborty, P., Liu, D., Zhang, R., Xu, Y., et al., 2013. A comparison study of atmospheric polycyclic aromatic hydrocarbons in three Indian cities using PUF disk passive air samplers. Atmos. Environ. 73, 16–21.

Cooper, W.J., Cramer, C.J., Martin, N.H., Mezyk, S.P., O'Shea, K.E., Cv, Sonntag, 2009. Free radical mechanisms for the treatment of methyl tert-butyl ether (MTBE) via advanced Oxidation/Reductive processes in aqueous solutions. Chem. Rev. 109, 1302–1345.

Croera, C., Ferrario, D., Gribaldo, L., 2008. In vitro toxicity of naphthalene, 1-naphthol, 2-naphthol and 1,4-naphthoquinone on human CFU-GM from female and male cord blood donors. Toxicol. in Vitro 22, 1555–1561.

Cui, H., Gu, X., Lu, S., Fu, X., Zhang, X., Fu, G.Y., et al., 2017a. Degradation of ethylbenzene in aqueous solution by sodium percarbonate activated with EDDS–Fe(III) complex. Chem. Eng. J. 309, 80–88.

Cui, J., Zhang, L., Xi, B., Zhang, J., Mao, X., 2017b. Chemical oxidation of benzene and trichloroethylene by a combination of peroxymonosulfate and permanganate linked by in-situ generated colloidal/amorphous MnO2. Chem. Eng. J. 313, 815–825.

Dai, Y., Wang, Y., Zuo, G., Kong, J., Guo, Y., Sun, C., et al., 2022. Photocatalytic degradation mechanism of phenanthrene over visible light driven plasmonic Ag/Ag3PO4/g-C3N4 heterojunction nanocomposite. Chemosphere 293, 133575.

Daifullah, A.H.A.M., Mohamed, M.M., 2004. Degradation of benzene, toluene ethylbenzene and p-xylene (BTEX) in aqueous solutions using UV/H2O2 system. J. Chem. Technol. Biotechnol. 79, 468–474.

David, B., 2009. Sonochemical degradation of PAH in aqueous solution. Part I: monocomponent PAH solution. Ultrason. Sonochem. 16, 260–265.

Deng, D., Lin, X., Ou, J., Wang, Z., Li, S., Deng, M., et al., 2015. Efficient chemical oxidation of high levels of soil-sorbed phenanthrene by ultrasound induced, thermally activated persulfate. Chem. Eng. J. 265, 176–183.

Dhar, K., Subashchandrabose, S.R., Venkateswarlu, K., Krishnan, K., Megharaj, M., 2020. Anaerobic microbial degradation of polycyclic aromatic hydrocarbons: a comprehensive review. In: de Voogt, P. (Ed.)Reviews of Environmental Contamination and Toxicologyvolume 251. Springer International Publishing, Cham, pp. 25–108.

Dias, I.N., Bassin, J.P., Dezotti, M., Vilar, V.J.P., 2018. Fluorene oxidation by solar-driven photo-Fenton process: toward mild pH conditions. Environ. Sci. Pollut. Res. 25, 27808–27818.

Dong, D., Li, P., Li, X., Xu, C., Gong, D., Zhang, Y., et al., 2010. Photocatalytic degradation of phenanthrene and pyrene on soil surfaces in the presence of nanometer rutile TiO2 under UV-irradiation. Chem. Eng. J. 158, 378–383.

Dong, C.-D., Chen, C.-W., Hung, C.-M., 2017a. Synthesis of magnetic biochar from bamboo biomass to activate persulfate for the removal of polycyclic aromatic hydrocarbons in marine sediments. Bioresour. Technol. 245, 188–195.

Dong, C.-D., Tsai, M.-L., Chen, C.-W., Hung, C.-M., 2017b. Heterogeneous persulfate oxidation of BTEX and MTBE using Fe3O4−CB magnetite composites and the cytotoxicity of degradation products. Int. Biodeterior. Biodegradation 124, 109–118.

Dong, C.-D., Tsai, M.-L., Chen, C.-W., Hung, C.-M., 2018. Remediation and cytotoxicity study of polycyclic aromatic hydrocarbon-contaminated marine sediments using synthesized iron oxide–carbon composite. Environ. Sci. Pollut. Res. 25, 5243–5253.

Dong, C.-D., Lu, Y.-C., Chang, J.-H., Wang, T.-H., Chen, C.-W., Hung, C.-M., 2019. Enhanced persulfate degradation of PAH-contaminated sediments using magnetic carbon microspheres as the catalyst substrate. Process Saf. Environ. Prot. 125, 219–227.

Eker, G., Hatipoglu, M., 2019. Effect of UV wavelength, temperature and photocatalyst on the removal of PAHs from industrial soil with photodegradation applications. Environ. Technol. 40, 3793–3803.

Elmobarak, W.F., Hameed, B.H., Almomani, F., Abdullah, A.Z., 2021. A review on the treatment of petroleum refinery wastewater using advanced oxidation processes. Catalysts 11, 782.

Falciglia, P.P., De Guidi, G., Catalfo, A., Vagliasindi, F.G.A., 2016. Remediation of soils contaminated with PAHs and nitro-PAHs using microwave irradiation. Chem. Eng. J. 296, 162–172.

Fatta-Kassinos, D., Vasquez, M.I., Kümmerer, K., 2011. Transformation products of pharmaceuticals in surface waters and wastewater formed during photolysis and advanced oxidation processes – degradation, elucidation of byproducts and assessment of their biological potency. Chemosphere 85, 693–709.

Fedorov, K., Plata-Gryl, M., Khan, J.A., Boczkaj, G., 2020. Ultrasound-assisted heterogeneous activation of persulfate and peroxymonosulfate by asphaltenes for the degradation of BTEX in water. J. Hazard. Mater. 397, 122804.

Fedorov, K., Sun, X., Boczkaj, G., 2021. Combination of hydrodynamic cavitation and SR-AOPs for simultaneous degradation of BTEX in water. Chem. Eng. J. 417, 128081.

Fernandes, A., Gagol, M., Makoś, P., Khan, J.A., Boczkaj, G., 2019. Integrated photocatalytic advanced oxidation system (TiO2/UV/O3/H2O2) for degradation of volatile organic compounds. Sep. Purif. Technol. 224, 1–14.

Fernandes, A., Makoś, P., Wang, Z., Boczkaj, G., 2020. Synergistic effect of TiO2 photocatalytic advanced oxidation processes in the treatment of refinery effluents. Chem. Eng. J. 391, 123488.

Fu, X., Gu, X., Lu, S., Miao, Z., Xu, M., Zhang, X., et al., 2015. Benzene depletion by Fe2 + -catalyzed sodium percarbonate in aqueous solution. Chem. Eng. J. 267, 25–33.

Fu, X., Gu, X., Lu, S., Sharma, V.K., Brusseau, M.L., Xue, Y., et al., 2017. Benzene oxidation by Fe(III)-activated percarbonate: matrix-constituent effects and degradation pathways. Chem. Eng. J. 309, 22–29.

Fu, J., Kyzas, G.Z., Cai, Z., Deliyanni, E.A., Liu, W., Zhao, D., 2018. Photocatalytic degradation of phenanthrene by graphite oxide-TiO2-Sr(OH)2/SrCO3 nanocomposite under solar

irradiation: effects of water quality parameters and predictive modeling. Chem. Eng. J. 335, 290–300.

Gągol, M., Przyjazny, A., Boczkaj, G., 2018a. Effective method of treatment of industrial effluents under basic pH conditions using acoustic cavitation – a comprehensive comparison with hydrodynamic cavitation processes. Chem. Eng. Process.- Process Intensif. 128, 103–113.

Gągol, M., Przyjazny, A., Boczkaj, G., 2018b. Highly effective degradation of selected groups of organic compounds by cavitation based AOPs under basic pH conditions. Ultrason. Sonochem. 45, 257–266.

Gao, S., Liang, J., Teng, T., Zhang, M., 2019. Petroleum contamination evaluation and bacterial community distribution in a historic oilfield located in loess plateau in China. Appl. Soil Ecol. 136, 30–42.

Gaurav, G.K., Mehmood, T., Kumar, M., Cheng, L., Sathishkumar, K., Kumar, A., et al., 2021. Review on polycyclic aromatic hydrocarbons (PAHs) migration from wastewater. J. Contam. Hydrol. 236, 103715.

Gavaskar, A., Condit, W., Harre, K., 2008. Cost and Performance Report for a Persulfate Treatability Study at Naval Air Station North Island. GRA and I. Gavaskar, A; Condit, W; Harre, K.

Guo, J., Gao, Q., Yang, S., Zheng, F., Du, B., Wen, S., et al., 2021. Degradation of pyrene in contaminated water and soil by Fe2 + -activated persulfate oxidation: performance, kinetics, and background electrolytes (Cl-, HCO3- and humic acid) effects. Process Saf. Environ. Prot. 146, 686–693.

Gupta, H., Gupta, B., 2015. Photocatalytic degradation of polycyclic aromatic hydrocarbon benzo[a]pyrene by iron oxides and identification of degradation products. Chemosphere 138, 924–931.

Hara, J., 2017. Oxidative degradation of benzene rings using iron sulfide activated by hydrogen peroxide/ozone. Chemosphere 189, 382–389.

Haygarth, K.S., Marin, T.W., Janik, I., Kanjana, K., Stanisky, C.M., Bartels, D.M., 2010. Carbonate radical formation in radiolysis of sodium carbonate and bicarbonate solutions up to 250 °C and the mechanism of its second order decay. J. Phys. Chem. A 114, 2142–2150.

Hung, C.-M., Chen, C.-W., Huang, C.-P., Dong, C.-D., 2021. Activation of peroxymonosulfate by nitrogen-doped carbocatalysts derived from brown algal (Sargassum duplicatum) for the degradation of polycyclic aromatic hydrocarbons in marine sediments. J. Environ. Chem. Eng. 9, 106420.

Hung, C.-M., Chen, C.-W., Huang, C.-P., Tsai, M.-L., Dong, C.-D., 2022. Metal-free carbocatalysts derived from macroalga biomass (Ulva lactuca) for the activation of peroxymonosulfate toward the remediation of polycyclic aromatic hydrocarbons laden marine sediments and its impacts on microbial community. Environ. Res. 208, 112782.

Hussain, A., Al-Barakah, F.N., Al-Sewailem, M., El-Saeid, M.H., Waqar, M., Ahmad, M., 2017. Oxidative photodegradation of pyrene and fluoranthene by Fe-based and Zn-based Fenton reagents. Sustainability 9, 870.

Iida, Y., Ashokkumar, M., Tuziuti, T., Kozuka, T., Yasui, K., Towata, A., et al., 2010. Bubble population phenomena in sonochemical reactor: I estimation of bubble size distribution and its number density with pulsed sonication – laser diffraction method. Ultrason. Sonochem. 17, 473–479.

Jia, H., Chen, H., Nulaji, G., Li, X., Wang, C., 2015. Effect of low-molecular-weight organic acids on photo-degradation of phenanthrene catalyzed by Fe(III)–smectite under visible light. Chemosphere 138, 266–271.

Jin, J., Sun, J., Lv, K., Guo, X., Liu, J., Bai, Y., et al., 2020. Oxygen-vacancy-rich BiO2–x/ Ag3PO4/CNT composite for polycyclic aromatic hydrocarbons (PAHs) removal via visible and near-infrared light irradiation. Ind. Eng. Chem. Res. 59, 5725–5735.

Kan, H., Wu, D., Wang, T., Qu, G., Zhang, P., Jia, H., et al., 2021. Crystallographic manganese oxides enhanced pyrene contaminated soil remediation in microwave activated persulfate system. Chem. Eng. J. 417, 127916.

Kang, H.-J., Lee, S.-Y., Kwon, J.-H., 2016. Physico-chemical properties and toxicity of alkylated polycyclic aromatic hydrocarbons. J. Hazard. Mater. 312, 200–207.

Ke, Y., Ning, X.-a., Liang, J., Zou, H., Sun, J., Cai, H., et al., 2018. Sludge treatment by integrated ultrasound-Fenton process: characterization of sludge organic matter and its impact on PAHs removal. J. Hazard. Mater. 343, 191–199.

Keith, L.H., 2015. The source of U.S. EPA's sixteen PAH priority pollutants. Polycycl. Aromat. Compd. 35, 147–160.

Khuman, S.N., Chakraborty, P., Cincinelli, A., Snow, D., Kumar, B., 2018. Polycyclic aromatic hydrocarbons in surface waters and riverine sediments of the Hooghly and Brahmaputra Rivers in the eastern and northeastern India. Sci. Total Environ. 636, 751–760.

Kohtani, S., Tomohiro, M., Tokumura, K., Nakagaki, R., 2005. Photooxidation reactions of polycyclic aromatic hydrocarbons over pure and Ag-loaded BiVO4 photocatalysts. Appl. Catal. B Environ. 58, 265–272.

Krichevskaya, M., Klauson, D., Portjanskaja, E., Preis, S., 2011. The cost evaluation of advanced oxidation processes in laboratory and pilot-scale experiments. Ozone Sci. Eng. 33, 211–223.

Krygowski, T.M., Ejsmont, K., Stępień, B.T., Cyrański, M.K., Poater, J., Solà, M., 2004. Relation between the substituent effect and aromaticity. J. Org. Chem. 69, 6634–6640.

Lai, X., Ning, X.-a., He, Y., Yuan, Y., Sun, J., Ke, Y., et al., 2019. Treatment of a simulated sludge by ultrasonic zero-valent iron/EDTA/Air process: interferences of inorganic salts in polyaromatic hydrocarbon removal. Waste Manag. 85, 548–556.

Lai, X., Ning, X.-a., Chen, J., Li, Y., Zhang, Y., Yuan, Y., 2020. Comparison of the Fe2 + /H2O2 and Fe2 + /PMS systems in simulated sludge: removal of PAHs, migration of elements and formation of chlorination by-products. J. Hazard. Mater. 398, 122826.

Lair, A., Ferronato, C., Chovelon, J.-M., Herrmann, J.-M., 2008. Naphthalene degradation in water by heterogeneous photocatalysis: an investigation of the influence of inorganic anions. J. Photochem. Photobiol. A Chem. 193, 193–203.

Lan, Y., Li, Z., Li, D., Yan, G., Yang, Z., Guo, S., 2019. Graphitic carbon nitride synthesized at different temperatures for enhanced visible-light photodegradation of 2-naphthol. Appl. Surf. Sci. 467–468, 411–422.

Lan, Y., Li, Z., Li, D., Xie, W., Yan, G., Guo, S., 2020. Visible-light responsive Z-scheme Bi@β-Bi2O3/g-C3N4 heterojunction for efficient photocatalytic degradation of 2,3-dihydroxynaphthalene. Chem. Eng. J. 392, 123686.

Lawal, A.T., 2017. Polycyclic aromatic hydrocarbons.A review. Cogent Environ. Sci. 3, 1339841.

Lee, J., Ashokkumar, M., Kentish, S., Grieser, F., 2005. Determination of the size distribution of sonoluminescence bubbles in a pulsed acoustic field. J. Am. Chem. Soc. 127, 16810–16811.

Lhotský, O., Krákorová, E., Mašín, P., Žebrák, R., Linhartová, L., Křesinová, Z., et al., 2017. Pharmaceuticals, benzene, toluene and chlorobenzene removal from contaminated groundwater by combined UV/H2O2 photo-oxidation and aeration. Water Res. 120, 245–255.

Li, W., Jain, T., Ishida, K., Liu, H., 2017. A mechanistic understanding of the degradation of trace organic contaminants by UV/hydrogen peroxide, UV/persulfate and UV/free chlorine for water reuse. Environ. Sci.: Water Res. Technol. 3, 128–138.

Li, L., Lai, C., Huang, F., Cheng, M., Zeng, G., Huang, D., et al., 2019. Degradation of naphthalene with magnetic bio-char activate hydrogen peroxide: synergism of bio-char and Fe–Mn binary oxides. Water Res. 160, 238–248.

Liang, C., Huang, C.-F., Chen, Y.-J., 2008. Potential for activated persulfate degradation of BTEX contamination. Water Res. 42, 4091–4100.

Lin, M., Ning, X.-a., An, T., Zhang, J., Chen, C., Ke, Y., et al., 2016. Degradation of polycyclic aromatic hydrocarbons (PAHs) in textile dyeing sludge with ultrasound and Fenton processes: effect of system parameters and synergistic effect study. J. Hazard. Mater. 307, 7–16.

Lin, Z., Shen, W., Chen, X., Corriou, J.-P., Xi, H., 2020. Impact of intermediate products on benzene photocatalytic oxidation in pulp mills: experimental and adsorption simulation study. Appl. Surf. Sci. 529, 147130.

Lin, M., Li, F., Cheng, W., Rong, X., Wang, W., 2022. Facile preparation of a novel modified biochar-based supramolecular self-assembled g-C3N4 for enhanced visible light photocatalytic degradation of phenanthrene. Chemosphere 288, 132620.

Liu, W., Sun, W., Borthwick, A.G.L., Ni, J., 2013. Comparison on aggregation and sedimentation of titanium dioxide, titanate nanotubes and titanate nanotubes-TiO2: influence of pH, ionic strength and natural organic matter. Colloids Surf. A Physicochem. Eng. Asp. 434, 319–328.

Liu, W., Lv, G., Sun, X., He, L., Zhang, C., Li, Z., 2019. Theoretical study on the reaction of anthracene with sulfate radical and hydroxyl radical in aqueous solution. Ecotoxicol. Environ. Saf. 183, 109551.

Luo, Z., Wang, J., Song, Y., Zheng, X., Qu, L., Wu, Z., et al., 2018. Remediation of phenanthrene contaminated soil by a solid state photo-Fenton reagent based on mesoporous magnetite/carboxylate-rich carbon composites and its phytotoxicity evaluation. ACS Sustain. Chem. Eng. 6, 13262–13275.

Ma, T., Wu, J., Mi, Y., Chen, Q., Ma, D., Chai, C., 2017. Novel Z-scheme g-C3N4/C@Bi2MoO6 composite with enhanced visible-light photocatalytic activity for β-naphthol degradation. Sep. Purif. Technol. 183, 54–65.

Ma, J., Yang, Y., Jiang, X., Xie, Z., Li, X., Chen, C., et al., 2018. Impacts of inorganic anions and natural organic matter on thermally activated persulfate oxidation of BTEX in water. Chemosphere 190, 296–306.

Makoś, P., Fernandes, A., Boczkaj, G., 2018. Method for the simultaneous determination of monoaromatic and polycyclic aromatic hydrocarbons in industrial effluents using dispersive liquid–liquid microextraction with gas chromatography–mass spectrometry. J. Sep. Sci. 41, 2360–2367.

Manariotis, I.D., Karapanagioti, H.K., Chrysikopoulos, C.V., 2011. Degradation of PAHs by high frequency ultrasound. Water Res. 45, 2587–2594.

Manassir, M., Pakiari, A.H., 2019. An electronic properties investigation to interpret the substituent constants of monosubstituted benzene derivatives. J. Mol. Graph. Model. 92, 201–207.

Monfort, O., Plesch, G., 2018. Bismuth vanadate-based semiconductor photocatalysts: a short critical review on the efficiency and the mechanism of photodegradation of organic pollutants. Environ. Sci. Pollut. Res. 25, 19362–19379.

Muff, J., Søgaard, E.G., 2010. Electrochemical degradation of PAH compounds in process water: a kinetic study on model solutions and a proof of concept study on runoff water from harbour sediment purification. Water Sci. Technol. 61, 2043–2051.

N. Mukwevho, N.K., Fosso-Kankeu, E., Waanders, F., Bunt, J., Ray, S.S., 2019. Visible light-excitable ZnO/2D graphitic-C3N4 heterostructure for the photodegradation of naphthalene. Desalin. Water Treat. 163, 10.

Nguyen, V.-H., Phan Thi, L.-A., Van Le, Q., Singh, P., Raizada, P., Kajitvichyanukul, P., 2020. Tailored photocatalysts and revealed reaction pathways for photodegradation of polycyclic aromatic hydrocarbons (PAHs) in water, soil and other sources. Chemosphere 260, 127529.

Oh, W.-D., Veksha, A., Chen, X., Adnan, R., Lim, J.-W., Leong, K.-H., et al., 2019. Catalytically active nitrogen-doped porous carbon derived from biowastes for organics removal via peroxymonosulfate activation. Chem. Eng. J. 374, 947–957.

Ong, W.-J., Tan, L.-L., Ng, Y.H., Yong, S.-T., Chai, S.-P., 2016. Graphitic carbon nitride (g-C3N4)-based photocatalysts for artificial photosynthesis and environmental remediation: are we a step closer to achieving sustainability? Chem. Rev. 116, 7159–7329.

Pardo, F., Santos, A., Romero, A., 2016. Fate of iron and polycyclic aromatic hydrocarbons during the remediation of a contaminated soil using iron-activated persulfate: a column study. Sci. Total Environ. 566–567, 480–488.

Peluffo, M., Pardo, F., Santos, A., Romero, A., 2016. Use of different kinds of persulfate activation with iron for the remediation of a PAH-contaminated soil. Sci. Total Environ. 563–564, 649–656.

Peyton, G.R., Glaze, W.H., 1988. Destruction of pollutants in water with ozone in combination with ultraviolet radiation. 3. Photolysis of aqueous ozone. Environ. Sci. Technol. 22, 761–767.

Rachna, Rani M., Shanker, U., 2018. Enhanced photocatalytic degradation of chrysene by Fe2O3@ZnHCF nanocubes. Chem. Eng. J. 348, 754–764.